

---

# EXTENSIONS OF HETEROGENEITY IN INTEGRATION AND PREDICTION (HIP) WITH R SHINY APPLICATION

---

A PREPRINT

**Jessica Butts, PhD**

Division of Biostatistics  
University of Minnesota Twin Cities

**Christine Wendt, MD**

Division of Pulmonary, Allergy and Critical Care  
University of Minnesota Twin Cities

**Russel Bowler, MD, PhD**

Division of Pulmonary, Critical Care and Sleep Medicine  
Department of Medicine  
National Jewish Health

**Craig P. Hersh, MD**

Channing Division of Network Medicine  
Brigham and Women's Hospital  
Harvard Medical School

**Qi Long, PhD**

Department of Biostatistics, Epidemiology and Informatics  
Perelman School of Medicine  
University of Pennsylvania

**Lynn Eberly, PhD**

Division of Biostatistics  
University of Minnesota Twin Cities

 **Sandra E. Safo\***

Division of Biostatistics  
University of Minnesota Twin Cities  
ssaf0@umn.edu

October 13, 2023

## ABSTRACT

Multiple data views measured on the same set of participants is becoming more common and has the potential to deepen our understanding of many complex diseases by analyzing these different views simultaneously. Equally important, many of these complex diseases show evidence of subgroup heterogeneity (e.g., by sex or race). HIP (Heterogeneity in Integration and Prediction) is among the first methods proposed to integrate multiple data views while also accounting for subgroup heterogeneity to identify common and subgroup-specific markers of a particular disease. However, HIP is applicable to continuous outcomes and requires programming expertise by the user. Here we propose extensions to HIP that accommodate multi-class, Poisson, and Zero-Inflated Poisson outcomes while retaining the benefits of HIP. Additionally, we introduce an R Shiny application, accessible on shinyapps.io at [https://multi-viewlearn.shinyapps.io/HIP\\_ShinyApp/](https://multi-viewlearn.shinyapps.io/HIP_ShinyApp/), that provides an interface with the Python implementation of HIP to allow more researchers to use the method anywhere and on any device. We applied HIP to identify genes and proteins common and specific to males and females that are associated with exacerbation frequency. Although some of the identified genes and proteins show evidence of a relationship with chronic obstructive pulmonary disease (COPD) in existing literature, others may be candidates for future research investigating their relationship with COPD. We demonstrate the use of the Shiny application with a publicly available data. An R-package for HIP would be made available at <https://github.com/lasandrall/HIP>.

**Keywords** Multi-view data; Subgroup Heterogeneity; Integrative Analysis; COPD; Multimodal; Multi-omics

---

\*Corresponding Author: Sandra E. Safo, [www.sandraesafo.com](http://www.sandraesafo.com)

## 1 Introduction

Chronic obstructive pulmonary disease (COPD) is a chronic disease affecting the lungs and airways in almost 4% of the global population in 2017 [Soriano et al., 2020]. Cigarette smoking is a known risk factor for COPD, but fewer than 50% of heavy smokers develop COPD [Agustí et al., 2023]. There are also many genetic and environmental factors influencing risk [Silverman, 2020, Hardin and Silverman, 2014, Hu et al., 2010, Chung and Adcock, 2008]. COPD research is further complicated by the subgroup heterogeneity that exists between males and females. In a meta-analysis, female smokers had a faster annual decline in forced expiratory volume in one second ( $FEV_1$ ) even if they smoked fewer cigarettes [Gan et al., 2006]. Another study found that women smokers generally had higher airway wall thickness (AWT) compared to male smokers [Kim et al., 2011]. Additionally, researchers found that women experienced increased risk of hospitalization for COPD compared to males even when controlling for smoking [Prescott et al., 1997].

The Genetic Epidemiology of COPD (COPDGene) Study [Regan et al., 2011] was designed to understand genetic factors related to the development of COPD. The study collected genetic and proteomic data on a subset of participants at the Phase 2 (P2) study visit. Given the availability of multi-view data (e.g., genomic and proteomic data) and the known subgroup heterogeneity between males and females, the application of an integrative analysis method accounting for subgroup heterogeneity to the COPDGene Study data offers the opportunity to gain new insights into COPD. Butts et al. [2023] recently proposed a method called HIP, short for Heterogeneity in Integration and Prediction, for integrating data from multiple sources and simultaneously predicting a *continuous* outcome while accounting for subgroup heterogeneity. HIP allows to identify *common* and *subgroup-specific* variables contributing most to the overall association among the views and the variation in the outcome. HIP was used to investigate airway wall thickness (AWT) as a proxy for COPD severity and the authors demonstrated that HIP was capable of identifying genes and proteins common and specific to males and females that were predictive of AWT. However, AWT is not the only way to characterize the effects of COPD, and one may be interested in different types of outcomes that are not continuous.

One such outcome of interest is the number of COPD exacerbations, generally defined as an acute worsening of symptoms that require a change in treatment; these symptoms can include cough, wheezing, dyspnea, chest tightness, and decreased exercise tolerance. While exacerbations vary in severity, severe cases may need to be hospitalized and put on a ventilator; patients who require ICU treatment have a 43-46% risk of death within a year of the hospitalization [Evenson, 2010]. As such the number of exacerbations experienced by patients is a clinically meaningful outcome. Additionally, the TORCH (Towards a Revolution in COPD Health) study found that females had a rate of exacerbations that was 25% higher than males during their 3-year follow-up [Celli et al., 2011]. This emphasizes not only the importance of looking at exacerbation frequency but also accounting for differences in sex. Because exacerbation frequency is a Poisson or rate variable, it is not compatible with the originally proposed HIP Butts et al. [2023].

Our goal is to deepen our investigation into the molecular underpinnings of sex differences in COPD mechanisms using data from the COPDGene Study [Regan et al., 2011] by identifying genes and proteins common and specific to males and females related to exacerbation frequency. For this analysis, we included COPDGene Study [Regan et al., 2011] participants with COPD (defined as GOLD stage  $\geq 1$ ) at P2 and with genomic, proteomic, and selected clinical covariates (age, BMI, race, pack-years,  $FEV_1\%$ , AWT, and % emphysema) available. Figure 1 shows the distributions of number of exacerbations in the past year for males and females in this subsample. First, we note a statistically significant difference in the number of events per person-year between males and females. Second, both males and females had several participants with zero exacerbations suggesting that a zero-inflated Poisson (ZIP) outcome may better fit this data.

To address our research goal, the simplest approach we could consider would be to use a penalized regression method such as the Elastic Net [Zou and Hastie, 2005] or Lasso [Tibshirani, 1994]. The `glmnet` package [Friedman et al., 2010] can implement the Lasso and Elastic Net on a binary or Poisson outcome, but these methods neither perform integrative analysis nor account for subgroup heterogeneity; they also cannot accommodate a ZIP outcome. These approaches would require concatenating data views as they can only accept a single data view; they would also require running separate analyses for each subgroup to allow for subgroup heterogeneity. These approaches are easily implemented but are not ideal for our research goal where we want to integrate data from multiple sources and associate these data with a ZIP outcome while accounting for subgroup heterogeneity.

There are several integrative analysis methods we could consider for this analysis, but to the best of our knowledge, none of them account for subgroup heterogeneity, and few can accommodate a ZIP outcome. For example, Canonical Variate Regression (CVR) [Luo et al., 2016] is a one-step method for simultaneously associating data from multiple sources and predicting a clinical outcome. CVR can accommodate continuous, binary or Poisson outcomes but not a ZIP outcome. Sparse Integrative Discriminant Analysis (SIDA) [Safo et al., 2021] is a one-step method for joint association and classification of data from multiple sources, but it is only applicable to classification problems (i.e., binary or multi-class

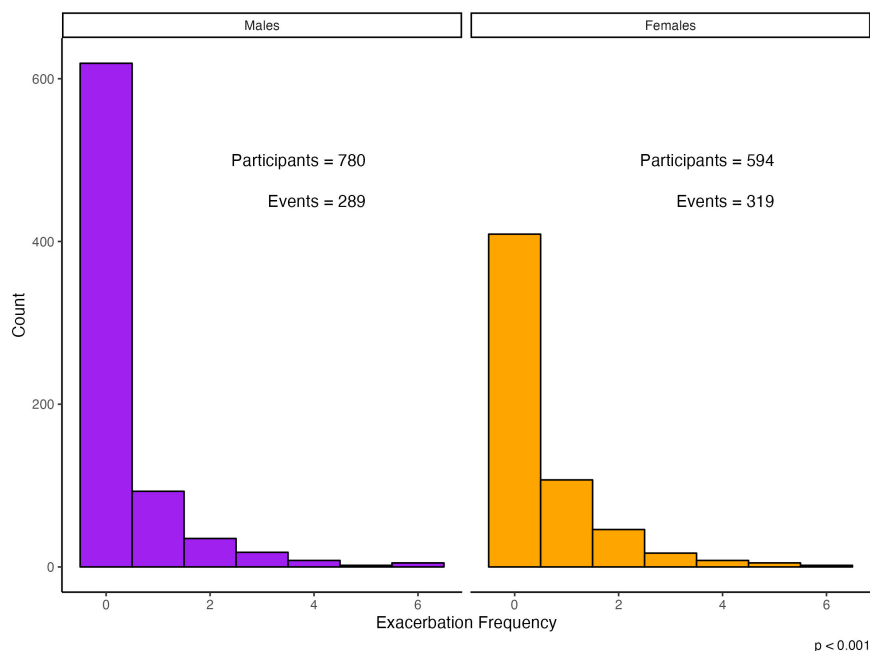


Figure 1: **Distribution of Exacerbation Frequency for Males and Females at COPDGene Study Visit P2.** The figure includes data from the P2 visit of the COPDGene Study for the subset of subjects included in our analysis. There is a statistically significant difference in the number of exacerbations experienced per person-year between males and females.

outcome). The aforementioned methods are one-step in that the problem of associating the multiple views are coupled with the problem of predicting an outcome. We could use a two-step method to first model the associations between views and then model the Poisson or ZIP response using information from the first step. For example, we could perform canonical correlation analysis (CCA) using SELP (Sparse Estimation through Linear Programming) [Safo et al., 2018] and then use the canonical variates as predictors in a Poisson or ZIP regression model. However, these all still fail to account for subgroup heterogeneity. To use any of these integrative analysis methods, we would have to either (a) concatenate the subgroups which ignores any potential subgroup heterogeneity or (b) run a separate analysis for each subgroup which limits power especially in a high-dimensional data setting where the sample size is typically less than the number of variables.

Alternatively, we could consider methods that account for subgroup heterogeneity, but to the best of our knowledge, none of them perform integrative analysis. One example is the Joint Lasso [Dondelinger et al., 2018], but this method is unable to accommodate a binary, Poisson, or ZIP outcome. More generally, methods that account for subgroup heterogeneity but do not perform integrative analysis would require either (a) concatenating data views within each subgroup which fails to model the associations between data views or (b) considering each view separately which fails to fully utilize the multi-view data and requires combining results post hoc.

With all of these existing methods, the only way to get subgroup-specific information is to fit the model separately on each subgroup, but this can greatly reduce the sample size and thus power to detect effects. Alternatively, if these methods are run on the combined subgroup data, the presence of any potential subgroup heterogeneity will be ignored. Existing methods do not fully utilize the available COPDGene Study [Regan et al., 2011] data to address our interest in identifying genes and proteins common and specific to males and females related to exacerbation frequency (modeled as a ZIP outcome). Thus, we propose extensions of HIP that can accommodate multi-class, Poisson, and ZIP outcomes while preserving the existing benefits of HIP (joint association and prediction method for integrative analysis accounting for subgroup heterogeneity and feature ranking) in order to identify common and subgroup-specific features predictive of an outcome. Further, since HIP requires Python programming expertise which is limiting, we develop a web application using the R Shiny framework and hosted on shinyapps.io, allowing HIP to be used anywhere, on any device, and by users with limited programming expertise. We believe that this will increase the widespread adoption of HIP by biomedical researchers interested in integrative analysis methods that also account for subgroup differences.

The remainder of this paper is structured as follows. In Section 2, we present the proposed methods to extend HIP. In Section 3, we describe the algorithmic implementation of this extension. In Section 4, we describe the design and results of simulations assessing the performance of HIP in comparison with existing methods. In Section 5, we apply HIP to data from the COPDGene Study [Regan et al., 2011] to examine the relationship of genes and proteins with exacerbation frequency. Section 6 introduces an R Shiny [Chang et al., 2023] application that provides a graphical interface to the underlying Python implementation of HIP. We conclude with discussion of limitations and future work in Section 7.

## 2 Methods

### 2.1 Notation and Problem

Consider the scenario where we have  $D$  data views (e.g., genomics, proteomics, clinical) measured on the same set of  $N$  subjects. Each view has  $p_d$  variables and  $S$  subgroups (known a priori). Each subgroup has sample size  $n_s$ . For our application,  $S = 2$  for biological sex (males and females). The total number of samples is  $N = \sum_{s=1}^S n_s$ . The data matrix for subgroup  $s$  is denoted by  $\mathbf{X}^{d,s} \in \mathcal{R}^{n_s \times p_d}$  where rows are for samples and columns are for variables. We define the outcome for each subgroup as  $\mathbf{Y}^s$ . For a multi-class outcome,  $\mathbf{Y}^s \in \mathcal{R}^{n_s \times m}$  with  $m$  being the number of classes, is an indicator matrix where each row has a one in the column corresponding to the class of the observation and a 0 in all other columns. For a Poisson or ZIP outcome,  $\mathbf{Y}^s \in \mathcal{R}^{n_s \times 2}$  where the first column is the observed counts and the second column is an offset. If no offset is provided, we add a column of ones as the offset which does not affect estimation.

### 2.2 Existing HIP Framework

Since we extend the original HIP to accommodate different types of outcomes beyond continuous outcome(s), we briefly introduce HIP for completeness sake. HIP simultaneously associates data from multiple views, predicts an outcome, and ranks or identifies common and subgroup-specific variables contributing to the overall dependency structure and the variation in an outcome by minimizing an objective function that is a sum of three terms: association term, hierarchical penalty term, and a prediction term. Consider the association term. HIP assumes that each view  $\mathbf{X}^{d,s}$  can be approximated by a product of low-rank view-independent matrix,  $\mathbf{Z}^s \in \mathcal{R}^{n_s \times K}$  and view-specific loadings  $\mathbf{B}^{d,s} \in \mathcal{R}^{p_d \times K}$ . That is, HIP assumes that  $\mathbf{X}^{d,s} = \mathbf{Z}^s \mathbf{B}^{d,sT} + \mathbf{E}^{d,s}$  where  $\mathbf{Z}^s$  are latent scores describing association across views and is shared by all views for subgroup  $s$ ,  $\mathbf{B}^{d,s} \in \mathcal{R}^{p_d \times K}$  are view and subgroup-specific variable loadings, and  $\mathbf{E}^{d,s}$  are errors as a result of approximating  $\mathbf{X}^{d,s}$  with  $\mathbf{Z}^s \mathbf{B}^{d,sT}$ . Here,  $K$  is the number of latent components, which is typically  $K \ll p_d$ , resulting in data dimensionality reduction. Then,  $\mathbf{B}^{d,s}$  and  $\mathbf{Z}^s$  are estimated to minimize the difference between the observed and estimated data via the loss function:

$$F(\mathbf{X}^{d,s}, \mathbf{Z}^s, \mathbf{B}^{d,s}) = \|\mathbf{X}^{d,s} - \mathbf{Z}^s \mathbf{B}^{d,sT}\|_F^2, \quad (1)$$

where  $\|\cdot\|_F$  is the Frobenius norm. We now consider the hierarchical penalty term which allows for identifying common and subgroup-specific variables. The hierarchical penalty implemented in HIP is a modified version of the penalty proposed in the Meta Lasso [Li et al., 2014]. For common and subgroup-specific variable selection, HIP decomposes  $\mathbf{B}^{d,s}$  into the element-wise product of  $\mathbf{G}^d$  and  $\mathbf{\Xi}^{d,s}$ , i.e.  $\mathbf{B}^{d,s} = \mathbf{G}^d \cdot \mathbf{\Xi}^{d,s}$ . Here,  $\mathbf{G}^d$  allows us to model common effects across subgroups while  $\mathbf{\Xi}^{d,s}$  allows us to model heterogeneity between subgroups. Since  $\mathbf{G}^d$  is common to all subgroups, its estimation allows us to borrow strength from all subgroups and improves power in estimation especially in high-dimensional settings where the number of samples is smaller than the number of variables. Of note, in this reparameterization, exact values of  $\mathbf{G}^d$  and  $\mathbf{\Xi}^{d,s}$  are not identifiable, but also are not directly needed for variable ranking since variable ranking is based on  $\mathbf{B}^{d,s}$ . HIP imposes a block  $L_{2,1}$  penalty on both  $\mathbf{G}^d$  and  $\mathbf{\Xi}^{d,s}$  which encourages selection of a variable in all  $K$  components or none of the components. Specifically, the hierarchical penalty term proposed in HIP is:

$$\sum_{d=1}^D \sum_{s=1}^S \mathcal{J}(\mathbf{B}^{d,s}) = \lambda_G \sum_{d=1}^D \gamma_d \sum_{l=1}^{p_d} \|\mathbf{g}_l^d\|_2 + \lambda_\xi \sum_{d=1}^D \gamma_d \sum_{s=1}^S \sum_{l=1}^{p_d} \|\xi_l^{d,s}\|_2, \quad (2)$$

where  $\mathbf{g}_l^d$  is a vector of length  $K$  in the  $l$ th row of  $\mathbf{G}^d$  and  $\xi_l^{d,s}$  is a vector of length  $K$  in the  $l$ th row of  $\mathbf{\Xi}^{d,s}$ . The strength of the penalty on  $\mathbf{G}^d$  and  $\mathbf{\Xi}^{d,s}$  is controlled by hyperparameters  $\lambda_G > 0$  and  $\lambda_\xi > 0$  respectively. The  $\gamma_d$  is a user-specified indicator of whether to penalize view  $d$ , i.e. whether to select variables in view  $d$ . This term is useful to force the inclusion of covariates believed to affect the outcome in the integrative analysis model.



We now consider the prediction term which relates the outcome to the association term via  $\mathbf{Z}^s$  using the loss function:  $F(\mathbf{Y}^s, \mathbf{Z}^s, \Theta, \beta_0) = \|\mathbf{Y}^s - \mathcal{J}_{n_s} \beta_0^T - \mathbf{Z}^s \Theta^T\|_F^2$ , where  $\Theta \in \mathcal{R}^{q \times K}$  is a matrix of regression coefficients,  $\mathcal{J}_{n_s}$  is a vector of ones of size  $n_s$  and  $\beta_0^T$  is a vector of length  $q$  for the intercept.  $\Theta$  is common and not subgroup-dependent. This allows the outcome data for all subgroups to be used in estimating the parameters and can improve the overall prediction of the outcome. Of note, for single continuous outcome,  $q = 1$ , and for multiple continuous outcome,  $q > 1$ . The presence of  $\mathbf{Z}^s$  in both the prediction and association terms is what allows HIP to be a one-step method. In other words, HIP simultaneously models the association between multiple views and predicts an outcome, compared to two-step methods that separate the association and prediction problems which may result in the  $\mathbf{Z}^s$  not being clinically meaningful. Since the two steps are combined in HIP, the estimation of the low-dimensional view-independent components  $\mathbf{Z}^s$  is guided by an outcome and therefore  $\mathbf{Z}^s$  is naturally endowed with prediction capabilities. Put together, HIP solves the following optimization problem to estimate the subgroup-specific view-independent components  $\mathbf{Z}^s$ , view-specific common variables  $\mathbf{G}^d$ , view- and subgroup-specific variables  $\Xi^{d,s}$  and regression coefficients  $\Theta$  that associate multiple views, predicts a continuous outcome(s) and identifies common- and subgroup-specific variables:

$$(\hat{\mathbf{B}}^{d,s}, \hat{\mathbf{Z}}^s, \hat{\Theta}, \hat{\beta}_0) = \min_{\mathbf{B}^{d,s}, \mathbf{Z}^s, \Theta, \beta_0} \sum_{s=1}^S F(\mathbf{Y}^s, \mathbf{Z}^s, \Theta, \beta_0) + \sum_{d=1}^D \sum_{s=1}^S F(\mathbf{X}^{d,s}, \mathbf{Z}^s, \mathbf{B}^{d,s}) + \sum_{d=1}^D \sum_{s=1}^S \mathcal{J}(\mathbf{B}^{d,s}) \quad (3)$$

Because the prediction term relies on the type of outcome, in the current work, we redefine  $F(\mathbf{Y}^s, \mathbf{Z}^s, \Theta, \beta_0)$  based on the type of outcome. We define  $F(\mathbf{Y}^s, \mathbf{Z}^s, \Theta, \beta_0)$  for multi-class, Poisson, and ZIP outcomes below.

## 2.3 Beyond Gaussian outcome(s): Modification of HIP Prediction Term

### 2.3.1 Multi-class Outcome

Similar to the continuous outcome, we relate the shared component  $\mathbf{Z}^s$  with the multi-class outcome. For this purpose, we use the cross-entropy loss function:  $F(\mathbf{Y}^s, \mathbf{Z}^s, \Theta, \beta_0) = -\sum_{i=1}^{n_s} \sum_{j=1}^m y_{ij}^s \log(a_{ij}^s)$ , where  $a_{ij}^s = \frac{\exp\{w_{ij}^s\}}{\sum_{j=1}^m \exp\{w_{ij}^s\}}$  is the *softmax* function generalizing logistic regression from binary to multi-class problems. Here,  $\mathbf{W}^s = \mathcal{J}_{n_s} \beta_0 + \mathbf{Z}^s \Theta$  represents scores,  $\mathcal{J}_{n_s}$  is an  $n_s \times 1$  matrix of ones,  $\Theta \in \mathcal{R}^{K \times m}$ , and  $w_{ij}^s$  is the  $ij$ th entry in  $\mathbf{W}^s$ . The *softmax* function forces the sum of each row in  $\mathbf{W}^s$  to be 1 so that each entry in the row represents a probability of case  $i$  belonging to class  $j$ .

### 2.3.2 Poisson Outcome

For a Poisson outcome, we define the prediction term:  $F(\mathbf{y}^s, \mathbf{Z}^s, \Theta, \beta_0) = \sum_{i=1}^{n_s} -y_i^s [\log(t_i^s) + \beta_0 + \mathbf{Z}_i^s \Theta] + t_i^s \exp(\beta_0 + \mathbf{Z}_i^s \Theta) + \log(y_i^s!)$ , which is based on the negative log-likelihood for a Poisson regression with an offset using a log link. Here,  $y_i^s$  is the outcome for the  $i$ th subject in subgroup  $s$ ,  $t_i^s$  is the offset for the  $i$ th subject in subgroup  $s$ , and  $\mathbf{Z}_i^s$  is the  $i$ th row of the  $\mathbf{Z}^s$  matrix. Here  $\Theta \in \mathcal{R}^{K \times 1}$  and  $\beta_0 \in \mathcal{R}^{1 \times 1}$ .

### 2.3.3 Zero-Inflated Poisson Outcome

As mentioned in Section 1, the motivating data set has a ZIP outcome rather than a true Poisson outcome. In order to accommodate this, we add an additional loss function to the code based on Lambert Lambert [1992]. In this model, the observed outcome is from the zero state with probability  $\tau$  and a Poisson random variable with probability  $1 - \tau$ . We assume that covariates are only related to the Poisson mean ( $\lambda$ ) and not  $\tau$ . Further, we assume that there is no relationship between  $\lambda$  and  $\tau$ . Thus,  $\log(\lambda_i) = \log(t_i) + \beta_0 + \mathbf{Z}_i^s \Theta$ . This assumption is a simplifying assumption, so while we could miss modeling a relationship that is there, it is not enforcing or requiring any specific constraints. Using this distribution, we use the negative log-likelihood to define the loss function as:

$$\begin{aligned} F(\mathbf{Y}^s, \mathbf{Z}^s, \Theta, \beta_0) = & \sum_{y_i^s=0} -\log(\exp[\tau] + \exp[-t_i^s \exp(\beta_0 + \mathbf{Z}_i^s \Theta)]) \\ & - \sum_{y_i^s>0} (y_i^s [\log(t_i^s) + \beta_0 + \mathbf{Z}_i^s \Theta] + t_i^s \exp[\beta_0 + \mathbf{Z}_i^s \Theta]) \\ & + \sum_{i=1}^{n_s} (\log(y_i^s!) + \log[1 + \exp(\tau)]). \end{aligned} \quad (4)$$

This does require estimation of the additional parameter  $\tau$  which is described in Section 3. Again  $\Theta \in \mathcal{R}^{K \times 1}$  and  $\beta_0 \in \mathcal{R}^{1 \times 1}$ .

## 2.4 Prediction

Suppose we have a test data,  $\mathbf{X}_{test}^{d,s}$ ,  $s = 1, \dots, S$ ,  $d = 1, \dots, D$ . Our goal in this section is to use the estimated optimization parameters  $\widehat{\mathbf{Z}}^s$ ,  $\widehat{\Theta}$ , and  $\widehat{\beta}_0$  and the test data  $\mathbf{X}_{test}^{d,s}$  to predict the test outcome  $\widehat{\mathbf{Y}}^s$  for subgroup  $s$ . We first estimate the test shared component for subgroup  $s$ ,  $\widehat{\mathbf{Z}}_{pred}^s$ , by solving the optimization problem:

$$\widehat{\mathbf{Z}}_{pred}^s = \min_{\mathbf{Z}^s} \sum_{d=1}^D \sum_{s=1}^S F(\mathbf{X}_{test}^{d,s}, \mathbf{Z}^s, \widehat{\mathbf{B}}^{d,s}) = \min_{\mathbf{Z}^s} \sum_{d=1}^D \sum_{s=1}^S \|\mathbf{X}_{test}^{d,s} - \mathbf{Z}^s \widehat{\mathbf{B}}^{d,sT}\|_F^2. \quad (5)$$

Let  $\mathbf{X}_{cat}^s$  be an  $n_s \times \{p_1 + \dots + p_d\}$  matrix that concatenates all  $D$  views for subgroup  $s$ , i.e.,  $\mathbf{X}_{cat}^s = [\mathbf{X}_{test}^{1,s}, \dots, \mathbf{X}_{test}^{D,s}]$ . Similarly, let  $\widehat{\mathbf{B}}_{cat} = [\widehat{\mathbf{B}}^{1,s}, \dots, \widehat{\mathbf{B}}^{D,s}]$  be a  $\{p_1 + \dots + p_d\} \times K$  matrix of variable coefficients. Then the solution to the optimization problem (5) is given as:  $\widehat{\mathbf{Z}}_{pred}^s = \mathbf{X}_{cat}^s \widehat{\mathbf{B}}_{cat}^s (\widehat{\mathbf{B}}_{cat}^s \widehat{\mathbf{B}}_{cat}^s)^{-1}$  for  $s = 1, \dots, S$ . Given the predicted  $\widehat{\mathbf{Z}}_{pred}^s$ , we predict the test outcome as follows:

$$\widehat{y}_i^s = \begin{cases} \arg \max_j \frac{\exp\{\widehat{w}_{ij}^s\}}{\sum_{j=1}^m \exp\{\widehat{w}_{ij}^s\}} & \text{Multi-class} \\ t_i^s \exp(\widehat{\beta}_0 + \widehat{\mathbf{Z}}_{pred_i}^s \widehat{\Theta}) & \text{Poisson} \\ (1 - \widehat{\tau}) t_i^s \exp(\widehat{\beta}_0 + \widehat{\mathbf{Z}}_{pred_i}^s \widehat{\Theta}) & \text{ZIP,} \end{cases}$$

where  $\widehat{\mathbf{Z}}_{pred_i}^s$  is the  $i$ th row of  $\widehat{\mathbf{Z}}_{pred}^s$ ,  $\widehat{w}_{ij}^s$  is the  $ij$ th element of  $\widehat{\mathbf{W}}^s = \mathcal{J}_{n_s} \widehat{\beta}_0 + \widehat{\mathbf{Z}}_{pred}^s \widehat{\Theta}$ .

## 3 Algorithm

### 3.1 Optimizing Parameters and Ranking Variables

We use alternating minimization algorithm to solve optimization problem (3). We initialize the entries of  $\mathbf{Z}^{s(0)}$  by randomly sampling from a  $U(0.9, 1.1)$  distribution. We initialize the entries of  $\mathbf{G}^{d(0)}$  for  $d = 1, \dots, D$ ,  $\Theta^{(0)}$ , and  $\beta_0^{(0)}$  with ones. We initialize  $\Xi^{d,s(0)}$  as  $\Xi^{d,s(0)} = [(\mathbf{Z}^{s(0)T} \mathbf{Z}^{s(0)})^{-1} \mathbf{Z}^{s(0)T} \mathbf{X}_{train}^{d,s}]^T$ .

We estimate  $\widehat{\mathbf{Z}}^s$  at iteration  $t$  by optimizing the following problem using gradient descent with gradients calculated using PyTorch Paszke et al. [2019]:

$$\widehat{\mathbf{Z}}^s{}^{(t)} = \min_{\mathbf{Z}^s} \sum_{s=1}^S F(\mathbf{Y}^s, \mathbf{Z}^s, \Theta^{(t-1)}, \beta_0^{(t-1)}) + \sum_{d=1}^D \sum_{s=1}^S \|\mathbf{X}^{d,s} - \mathbf{Z}^s \mathbf{B}^{d,s(t-1)T}\|_F^2, \quad (6)$$

where  $F(\mathbf{Y}^s, \mathbf{Z}^s, \Theta^{(t-1)}, \beta_0^{(t-1)})$  depends on the type of outcome. We use FISTA (fast iterative shrinkage-thresholding algorithm) with backtracking Beck and Teboulle [2009] to speed up convergence and select an appropriate step size. For a ZIP outcome, further consideration has to be given to the additional parameter,  $\tau$ . The parameter  $\tau$  is the probability that a given observation is in the zero state. Note that this differs from  $P(y_i^s = 0) = \tau + (1 - \tau)e^{-\lambda_i}$  as  $P(y_i^s = 0)$  includes the probability that is in the zero state plus the probability of a zero from a Poisson distribution with mean  $\lambda_i$ . We initialize  $\tau$  using the observed proportion of excess 0s beyond the proportion predicted by the Poisson model across all observations [Lambert, 1992] shown in (7). Specifically, the first term is the observed proportion of zeros, and the second term is the  $P(y_i^s = 0 | \lambda_i = \beta_0 + \mathbf{Z}_i^s \Theta)$  averaged across all observations. In the sub-optimizations for  $\mathbf{Z}^s$  and  $\Theta/\beta_0$ ,  $\tau$  is treated as a fixed value. Once all other model estimates have been updated,  $\tau$  is recalculated with the current model estimates of  $\mathbf{Z}^s$ ,  $\Theta$ , and  $\beta_0$  as:

$$\widehat{p}_0 = \frac{\sum_{s=1}^S \sum_{i=1}^{n_s} I(y_i^s = 0) - \sum_{s=1}^S \sum_{i=1}^{n_s} \exp[-\exp(\beta_0 + \mathbf{Z}_i^s \Theta)]}{\sum_{s=1}^S n_s}. \quad (7)$$

To estimate  $\mathbf{B}^{d,s(t)}$ , we first estimate  $\mathbf{G}^{d(t)}$  for each of the  $D$  data views. For a fixed  $\Xi^{d,s(t-1)}$ , we solve the following optimization problem using using the Adagrad Duchi et al. [2011] optimizer in PyTorch Paszke et al. [2019]:

$$\widehat{\mathbf{G}}^{d(t)} = \min_{\mathbf{G}^d \in \mathbb{R}^{p_d \times K}} \sum_{s=1}^S \|\mathbf{X}^{d,s} - \mathbf{Z}^{s(t)} (\mathbf{G}^d \cdot \Xi^{d,s(t)})^T\|_F^2 + \lambda_G \gamma_d \sum_{l=1}^{p_d} \|\mathbf{g}_l^d\|_2. \quad (8)$$

Convergence is defined as the relative change in (8) evaluated at  $\hat{\mathbf{G}}^{d^{(t)}}$  and  $\hat{\mathbf{G}}^{d^{(t-1)}}$ . We then use these updated estimates for  $\mathbf{Z}^s$  and  $\mathbf{G}^d$  to estimate  $\Xi^{d,s^{(t)}}$  by solving the optimization problem:

$$\hat{\Xi}^{d,s^{(t+1)}} = \min_{\Xi^{d,s} \in \mathbb{R}^{p_d \times K}} \|(\mathbf{X}^{d,s} - \mathbf{Z}^{s^{(t)}} (\mathbf{G}^{d^{(t)}} \cdot \Xi^{d,s})^T)\|_F^2 + \lambda_\xi \gamma_d \sum_{l=1}^{p_d} \|\xi_l^{d,s}\|_2. \quad (9)$$

We use the same technique described for the optimization of  $\mathbf{G}^d$  with an analogous convergence criterion defined as the relative change in (9) evaluated at  $\hat{\Xi}^{d,s^{(t)}}$  and  $\hat{\Xi}^{d,s^{(t-1)}}$ .

We note that because we use an automatic differentiation algorithm, the  $L_{2,1}$  (or block  $l_2/l_1$ ) penalty does not result in zero coefficients. However, the magnitude of the coefficients in  $\hat{\mathbf{B}}^{d,s}$  for the noise variables are clearly smaller than the coefficients of the signal variables. Thus, we rank and identify relevant variables based on the magnitude of the  $L_2$  norm of the rows in  $\hat{\mathbf{B}}^{d,s}$ . In implementing the ranking procedure, the user specifies the number of variables (denote as  $N_{top}$ ) they wish to keep, which could vary across data views. We run Algorithm 1 on the full training data and select the  $N_{top}$  variables for each view and subgroup based on the estimated  $\mathbf{B}^{d,s}$ . Then, we run Algorithm 1 a second time but with the selected variables. The estimated parameters based on this ‘subset’ of data are used in the prediction procedure described in section 2.4.

We estimate  $\Theta$  and  $\beta_0$  using  $\hat{\mathbf{Z}}^s{}^{(t)}$  to optimize the equation problem:

$$(\hat{\Theta}^{(t)}, \hat{\beta}_0^{(t)}) = \min_{\Theta, \beta_0} \sum_{s=1}^S F(\mathbf{Y}^s, \mathbf{Z}^{s^{(t)}}, \Theta, \beta_0).$$

We use ISTA (iterative shrinkage-thresholding algorithm) with backtracking Beck and Teboulle [2009] to select an appropriate step size. The convergence criterion is the relative change in (3.1) evaluated at  $\hat{\Theta}^{(t)}, \hat{\beta}_0^{(t)}$  and  $\hat{\Theta}^{(t-1)}, \hat{\beta}_0^{(t-1)}$ .

### 3.2 Tuning Parameters

The optimization problem depends on  $\lambda = (\lambda_G, \lambda_\xi)$  and  $K$ . We use grid and random Bergstra and Bengio [2012] searches for selecting  $\lambda$ , and we follow the automatic or scree plot approaches to selecting  $K$  described in Butts et al. [2023]. However, we include eBIC (extended Bayesian Information Criterion) [Chen and Chen, 2008] as an additional model selection criterion. This criterion modifies the priors used in the traditional BIC (Bayesian Information Criterion) to prevent larger probabilities being assigned to models with more covariates. If we consider the set of models with  $q$  covariates  $\mathcal{M}_q$ , then for the  $j^{th}$  model  $\mathcal{M}_{qj} \in \mathcal{M}_q$  with maximum likelihood estimated parameters  $\hat{\theta}(\mathcal{M}_{qj})$ , eBIC is defined as

$$eBIC_\delta(\mathcal{M}_{qj}) = -2 \log \mathcal{L}_n(\hat{\theta}(\mathcal{M}_{qj})) + \nu(\mathcal{M}_{qj}) \log(n) + 2\delta \log(\kappa(\mathcal{M}_q))$$

for  $0 \leq \delta \leq 1$  where  $\nu(\mathcal{M}_{qj})$  is the number of estimated parameters,  $\kappa(\mathcal{M}_q)$  is the number of models in  $\mathcal{M}_q$ , and  $n$  is the number of observations. When  $\delta = 0$ , eBIC is equivalent to the standard BIC, and  $\delta = 1$  ensures consistency when the number of covariates is very large.

The eBIC criterion for HIP is defined in (10). We use  $F(\mathbf{Y}^s, \hat{\mathbf{Z}}^s, \hat{\Theta}, \hat{\beta}_0)$  in the first term as it is proportional to the log-likelihood. For the number of parameters  $\nu$ , we count the number of variables that will be included in the subset model fit for HIP. A variable is included in the subset fit if it is one of the  $N_{top}$  variables selected in at least one subgroup, where  $N_{top}$  is user-specified (e.g., top 10% of variables or top 50 variables) and can vary by data view. Thus, we define  $\nu(\hat{\mathbf{B}}) = \sum_{d=1}^D \sum_{l=1}^{p_d} I(\hat{\mathbf{B}}_l^{d,s} \in N_{top} \text{ for any } s = 1, \dots, S)$ ; note this value is the same for all subgroups. For the number of models in  $\mathcal{M}_q$ , we note that in a given view, we could include as few as  $N_{top}$  variables in the case where all subgroups select the same set of variables and as many as  $S * N_{top}$  variables when all subgroups select distinct sets of variables. Thus, to count the size of  $\mathcal{M}_q$  where  $q = N_{top}$ , we sum the combinations of choosing each possibility between  $N_{top}$  and  $S * N_{top}$  from the  $p_d$  variables in the view. The code will return values for  $eBIC_0$ ,  $eBIC_{0.5}$ , and  $eBIC_1$ :

$$eBIC_\delta = 2 \sum_{s=1}^S F(\mathbf{Y}^s, \hat{\mathbf{Z}}^s, \hat{\Theta}, \hat{\beta}_0) + \sum_{s=1}^S \log(n_s) \nu(\hat{\mathbf{B}}) + 2\delta \sum_{d=1}^D \log \left[ \sum_{w=N_{top}}^{S * N_{top}} \binom{p_d}{w} \right] \quad (10)$$

**Algorithm 1** Overview of Optimization Algorithm

---

```

Initialize  $\mathbf{Z}^{s(0)}$ ,  $\boldsymbol{\theta}^{(0)}$ ,  $\beta_0^{(0)}$ ,  $\mathbf{G}^{d(0)}$ , and  $\Xi^{d,s(0)}$ 
if family = 'ZIP' then
  Initialize  $\tau^{(0)} = \frac{\sum_{s=1}^S \sum_{i=1}^{n_s} I(y_i^s=0) - \sum_{s=1}^S \sum_{i=1}^{n_s} \exp[-\exp(\beta_0^{(0)} + \mathbf{Z}_i^{s(0)} \boldsymbol{\theta}^{(0)})]}{\sum_{s=1}^S n_s}$ 
end if
for  $t = 1, \dots, iter_{max}$  do
  for  $s = 1, \dots, S$  do
     $\mathbf{Z}^{s(t)} \leftarrow \arg \min_{\mathbf{Z}^s} \left[ F(\mathbf{Y}^s, \mathbf{Z}^{s(t-1)}, \beta_0^{(t-1)}, \boldsymbol{\theta}^{(t-1)}, \tau^{(t-1)}) + \sum_{d=1}^D F(\mathbf{X}^{d,s}, \mathbf{Z}^{s(t-1)}, \mathbf{G}^{d(t-1)}, \Xi^{d,s(t-1)}) \right]$ 
    Standardize columns of  $\mathbf{Z}^{s(t)}$  to have mean 0 and variance 1
  end for
  for  $d = 1, \dots, D$  do
     $\mathbf{G}^{d(t)} \leftarrow \arg \min_{\mathbf{G}^d} \sum_{s=1}^S F(\mathbf{X}^{d,s}, \mathbf{Z}^{s(t)}, \mathbf{G}^{d(t-1)}, \Xi^{d,s(t-1)}) + \lambda_g \sum_{l=1}^{p_d} \|g_l^d\|_2$ 
    for  $s = 1, \dots, S$  do
       $\Xi^{d,s(t)} \leftarrow \arg \min_{\Xi^{d,s}} F(\mathbf{X}^{d,s}, \mathbf{Z}^{s(t)}, \mathbf{G}^{d(t)}, \Xi^{d,s(t-1)}) + \lambda_\xi \sum_{l=1}^{p_d} \|\xi_l^{d,s}\|_2$ 
    end for
  end for
   $\boldsymbol{\theta}^{(t)}, \beta_0^{(t)} \leftarrow \arg \min_{\boldsymbol{\theta}, \beta_0} \sum_{s=1}^S F(\mathbf{Y}^s, \mathbf{Z}^{s(t)}, \beta_0^{(t-1)}, \boldsymbol{\theta}^{(t-1)}, \tau^{(t-1)})$ 
  if family = 'ZIP' then
     $\tau^{(t)} = \frac{\sum_{s=1}^S \sum_{i=1}^{n_s} I(y_i^s = 0) - \sum_{s=1}^S \sum_{i=1}^{n_s} \exp[-\exp(\beta_0^{(t)} + \mathbf{Z}_i^{s(t)} \boldsymbol{\theta}^{(t)})]}{\sum_{s=1}^S n_s}$ 
  end if
  if Relative Loss  $< \epsilon$  then
    Declare convergence and return estimates
  else if  $t = iter_{max}$  then
    Return estimate with warning
  end if
end for

```

---

## 4 Simulations

### 4.1 Set-up

Simulations were run for binary, Poisson, and ZIP outcomes. For all outcomes, there were two views and two subgroups, i.e.,  $D = S = 2$ , and there were  $n_1 = 250$  subjects belonging to the first subgroup and  $n_2 = 260$  subjects belonging to the second subgroup. We considered two different scenarios for degree of subgroup heterogeneity: Full Overlap and Partial Overlap. In both scenarios, there are 50 variables important to each subgroup for each view. In the Full Overlap scenario, the 50 important variables are the same for both subgroups; in the Partial Overlap scenario, 25 of the important variables are common to both subgroups and 25 are unique to each subgroup. For each of the outcomes and scenarios, there were two different sets of variable dimensions in the data views. In the low dimensional setting, the first data set had  $p_1 = 300$  variables, and the second had  $p_2 = 350$ . In the high dimensional setting, the first data set had  $p_1 = 2000$  variables, and the second had  $p_2 = 3000$  variables.

### 4.2 Data Generation

The data were generated following a process based on Luo et al. [Luo et al., 2016]. Entries in rows of  $\mathbf{B}^{d,s}$  corresponding to a signal variable were drawn from a  $U(-1, -0.5) \cup U(0.5, 1)$ ; otherwise the entry was set to 0. The columns of each  $\mathbf{B}^{d,s}$  were then orthonormalized using a QR decomposition. The entries of  $\mathbf{Z}^s$  are drawn from  $N(\mu = 25.0, \sigma = 3.0)$  and entries of  $\mathbf{E}^{d,s}$  from  $N(\mu = 0.0, \sigma = 1.0)$ . Then the covariate matrices  $\mathbf{X}^{d,s}$  are formed as  $\mathbf{Z}^s \mathbf{B}^{d,s^T} + \mathbf{E}^{d,s}$ .

At this point, the processes diverge somewhat for the different outcomes. For the binary outcome, we apply the *softmax* function to  $\mathbf{W}^s = \mathcal{J}_{n_s} \beta_0 + \mathbf{Z}^s \boldsymbol{\theta} + \mathbf{E}_y^s$  where  $\mathcal{J}_{n_s}$  is an  $n_s \times 1$  matrix of ones,  $\mathbf{E}_y^s$  is an  $n_s \times 2$  matrix of standard normal errors and assign the class with the largest probability for each observation. Here  $\beta_0 = [0.5 \quad 0.5]$

and  $\Theta = \begin{bmatrix} 1.0 & 0.5 \\ 0.2 & 0.8 \end{bmatrix}$ . For the Poisson and ZIP outcomes, we first standardize the columns of  $\mathbf{Z}^s$  to have mean 0 and variance 1. The observations are then generated from the Pytorch [Paszke et al., 2019] Poisson random variable generator with mean  $\exp(\mathcal{J}_{n_s}\beta_0 + \mathbf{Z}^s\Theta)$ , i.e., observation  $y_i^s \sim \text{Poisson}(\exp(\beta_0 + \mathbf{Z}_i^s\Theta))$ . Here  $\beta_0 = 2.0$  and  $\Theta = [0.7 \ 0.2]^T$ . For the ZIP outcome, each observation is then multiplied by a draw from a Bernoulli distribution that is 0 with probability  $\tau = 0.25$ .

### 4.3 Comparison Methods

For all outcomes under consideration (binary, Poisson, and ZIP), we are unaware of any other methods that perform integrative analysis while also accounting for subgroup heterogeneity. For the binary outcome, we compare HIP to two integrative analysis methods: CVR [Luo et al., 2016] as implemented in the R package CVR [Luo and Chen, 2017] and SIDA [Safo et al., 2021] as implemented in the R package `mvlearnR` [Safo and Palzer, 2022]. Because neither of these methods accounts for subgroup heterogeneity, we implement each method two ways: (1) all subgroups concatenated within each view (Concatenated) and (2) a separate model for each subgroup (Subgroup). We also compare HIP to the Lasso [Tibshirani, 1994] and the Elastic Net [Zou and Hastie, 2005] as implemented in the R package `glmnet` [Friedman et al., 2010]. Neither of these two methods perform integrative analysis, so the two views are concatenated for these methods. We again implement two ways: (1) concatenating the subgroups (Concatenated) and (2) separate models for each subgroup (Subgroup).

For the Poisson outcome, SIDA is no longer applicable, so we instead compare HIP to the two-step integrative analysis method SELPCCA [Safo et al., 2018] as implemented in the R package `mvlearnR` [Safo and Palzer, 2022]. Since SELPCCA does not account for subgroup heterogeneity, we again fit concatenated and subgroup models (Concatenated SELPCCA and Subgroup SELPCCA, respectively).

For the ZIP outcome, CVR, Lasso, and Elastic Net cannot explicitly account for a ZIP outcome, but we still fit these models using a Poisson family. We also fit HIP specifying a Poisson outcome [HIP (Grid)-Poisson and HIP (Random)-Poisson] to demonstrate the importance of accounting for the zero-inflated nature of the data. Finally, because SELPCCA is a two-step method, we use the canonical variables from SELPCCA in a ZIP regression model fit with the `zeroinfl` function [Zeileis et al., 2008] in R package `pscl` [Jackman, 2020]. We again fit a model on the concatenated subgroups (Concatenated SELPCCA-ZIP) and separate models for each subgroup (Subgroup SELPCCA-ZIP).

Tuning parameters for the comparison methods were selected using 10-fold cross-validation. For the Elastic Net, we set  $\alpha = 0.5$ . Tuning parameters for HIP were selected using  $eBIC_1$ ; we considered a range of  $(0, 2]$  for  $\lambda_\xi$  and  $\lambda_G$  with 8 steps for each. The true values for  $K$  (i.e., 2) and  $N_{top}$  (i.e., 50) were used for all simulations.

### 4.4 Evaluation Measures

We compare HIP to the existing methods in terms of variable selection and prediction ability for new data. For variable selection, we will estimate the true positive rate ( $\text{TPR} = \frac{\text{True Positives}}{\text{True Positives} + \text{False Negatives}}$ ), false positive rate ( $\text{FPR} = \frac{\text{False Positives}}{\text{True Negatives} + \text{False Positives}}$ ), and F1 score ( $\text{F1} = \frac{\text{True Positives}}{\text{True Positives} + \frac{1}{2}(\text{False Positives} + \text{False Negatives})}$ ) which are all constrained to be between 0 and 1. Ideally, TPR and F1 are 1 and FPR is 0.

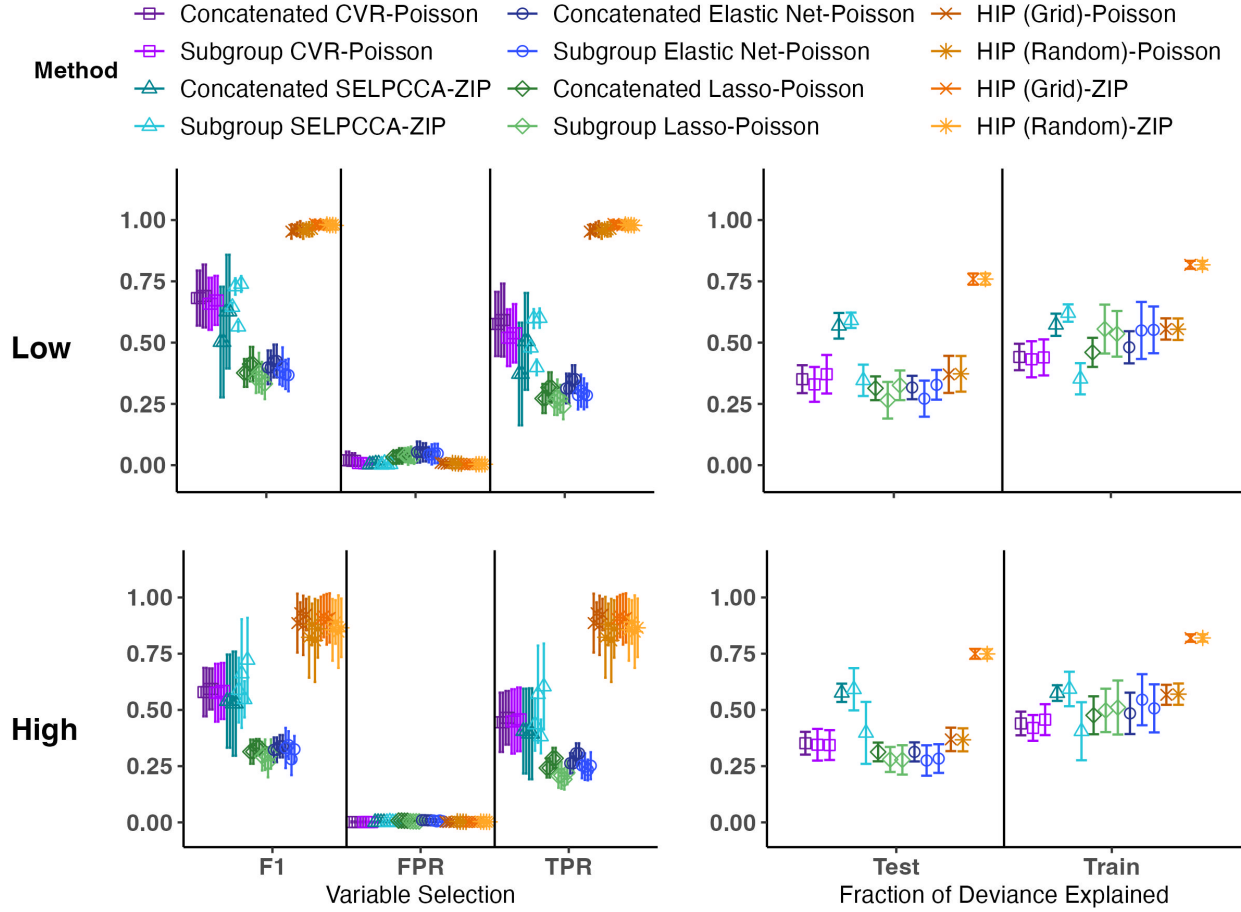
To compare predictive ability for the binary outcome, we look at classification accuracy, and for both Poisson and ZIP outcomes, we look at the fraction of deviance explained,  $D^2 = \frac{D_{null} - D_{opt}}{D_{null}}$ , where  $D_{null}$  is the deviance of the null model and  $D_{opt}$  is the deviance of the model with optimal tuning parameters [Hastie et al., 2016]. Results are averaged over 20 Monte Carlo data sets.

### 4.5 Results

We focus on the results for the ZIP outcome here as the motivating data have a ZIP outcome; results for the ZIP outcome with Full Overlap scenario as well as binary and Poisson outcomes are presented in the supplemental information (Figures S1 - S8).

First, we note the performance of HIP (Grid) and HIP (Random) are very similar in both the low and high dimensional settings for both the Full and Partial Overlap scenarios (Figures 2 and 3 respectively), so we recommend the use of HIP (Random) as it is computationally faster. In terms of variable selection, HIP (Grid) and HIP (Random) show the highest TPR and F1 values; all methods show low FPRs. The ZIP model only improves variable selection slightly over the HIP Poisson fits. The other two integrative methods, CVR and SELPCCA-ZIP, show similar variable selection performance to each other and show a benefit over the non-integrative methods (Elastic Net and Lasso), but they do not perform

Figure 2: **Results for ZIP Outcome, Full Overlap Scenario.** The first row corresponds to the low dimension ( $p_1 = 300, p_2 = 350$ ) and the second to the high dimension ( $p_1 = 2000, p_2 = 3000$ ). For all settings,  $n_1 = 250$  and  $n_2 = 260$ . The right column is the fraction of deviance explained ( $D^2$ ), so a higher value indicates better performance. Results are mean  $\pm$  one standard deviation summarized across 20 generated data sets.

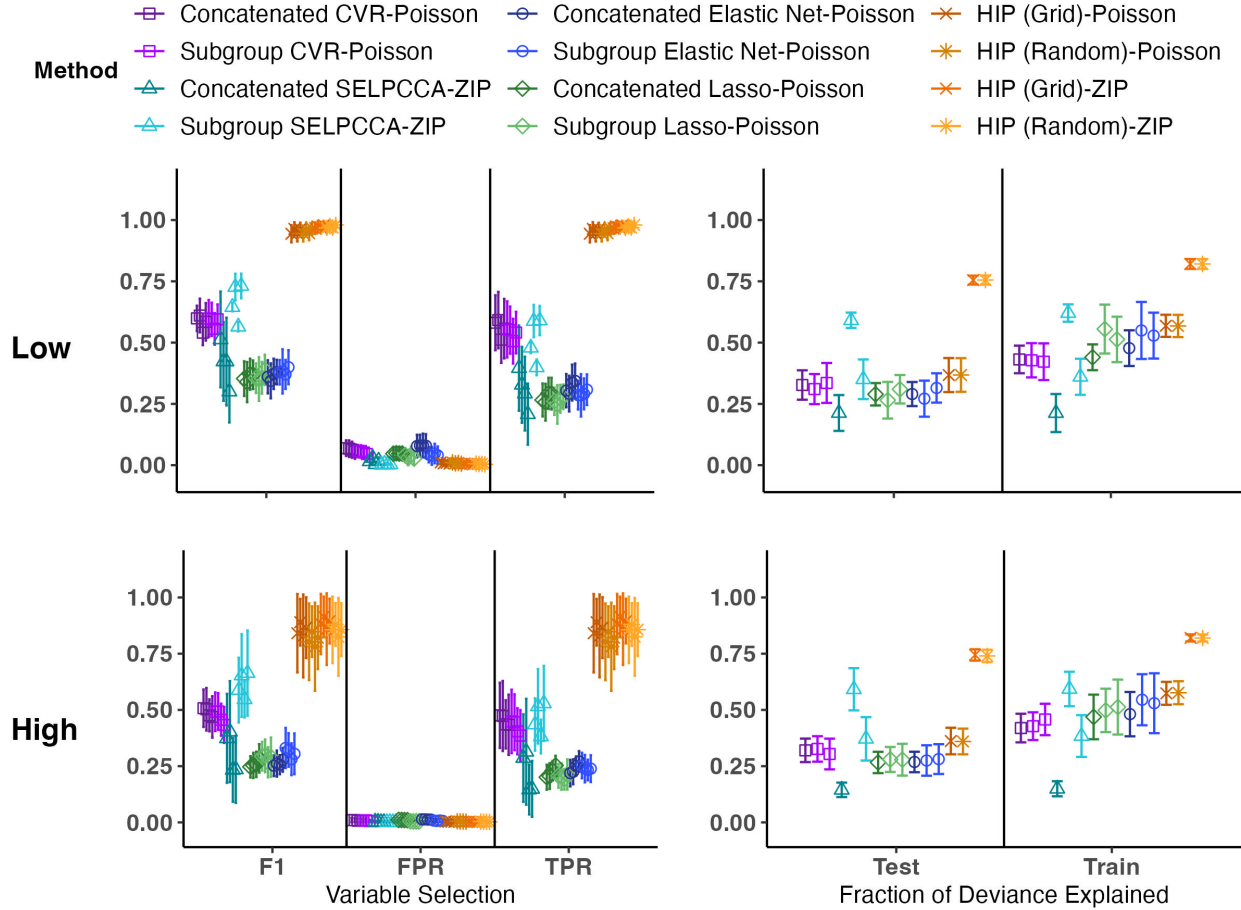


nearly as well as HIP. All of the comparison methods seem to be missing many of the true signal variables as evidenced by lower TPRs.

In terms of predictive ability in the Full Overlap Scenario, we note that HIP and the SELPCCA-ZIP models have a much higher fraction of deviance explained than the methods that do not account for the zero-inflated nature of the data, highlighting the importance of doing so. In the Partial Overlap Scenario, Concatenated SELPCCA-ZIP has a much lower  $D^2$  than in the Full Overlap Scenario suggesting that this method has more difficulty when subgroup heterogeneity exists in the data. HIP has the highest fraction of deviance explained out of all methods applied for both the low and high dimensional settings in both the Full and Partial Overlap Scenarios indicating HIP is still favorable even if subgroup heterogeneity does not exist in the data.

Computation times for all methods are summarized for the Full and Partial Overlap Scenarios in Supplemental Figures S9 and S10 respectively. The Lasso and Elastic net are the fastest in all scenarios, but because these methods do not perform integrative analysis or account for subgroup heterogeneity, the variable selection and predictive ability suffers. Of the methods that perform integrative analysis, HIP (Random) is consistently the fastest with larger computational advantages in the high dimensional setting particularly when compared to CVR. Concatenated SELPCCA-ZIP has similar computation times as HIP (Random) in the Partial Overlap setting, but this is the setting where the performance of Concatenated SELPCCA-ZIP was reduced dramatically.

Figure 3: **Performance Results for ZIP Outcome, Partial Overlap Scenario.** The first row corresponds to the low dimension ( $p_1 = 300, p_2 = 350$ ) and the second to the high dimension ( $p_1 = 2000, p_2 = 3000$ ). For all settings,  $n_1 = 250$  and  $n_2 = 260$ . The right column is the fraction of deviance explained ( $D^2$ ), so a higher value indicates better performance. Results are mean  $\pm$  one standard deviation summarized across 20 generated data sets.



## 5 Application to Exacerbation Frequency

### 5.1 Goals

In this section, our goal is to use the genetic and proteomic data from the COPDGene Study [Regan et al., 2011] in combination with clinical data to gain new insights into the molecular architecture of COPD in males and females. To be included in the analyses, participants had to have COPD at P2 (defined as GOLD stage  $\geq 1$ ) and have proteomic, genomic, and selected clinical covariates (age, BMI, race, pack-years, FEV<sub>1</sub>%, AWT, and % emphysema) available. There were  $N = 1374$  participants meeting these criteria with  $n_1 = 780$  males and  $n_2 = 594$  females; demographic characteristics of this sample are in Table 1. Continuous variables were compared between males and females using t-tests and categorical variables using  $\chi^2$  tests. Participants were predominantly non-Hispanic white; there were not statistically significant sex differences in age, BMI, BODE index, percentage of current smokers, or percentage with diabetes. Males and females differed in their exacerbation frequency ( $p < 0.001$ ) but did not have significantly different lung function as measured by mean FEV<sub>1</sub>% predicted. Given the available data, and the sex differences in exacerbation frequency, we first identify genes and proteins common and specific to males and females associated with exacerbation frequency. Using those identified genes and proteins, we then explore pathways enriched for males and females.

### 5.2 Applying HIP and Existing Methods

The COPDGene data includes 19263 genes and 4979 proteins. We first performed unsupervised filtering to select the 5000 genes and 2000 proteins with the largest variances. To preserve as much generalizability as possible, we then

Table 1: **Characteristics of Participants Included in COPDGene Application.** All measurements are from the Year 5 study visit to align with the collection of proteomic and genomic data.

Variable	Males N = 780	Females N = 594	P-value
Age	68.29 (8.35)	68.03 (8.36)	0.564
BMI	28.03 (5.62)	27.69 (6.59)	0.318
FEV <sub>1</sub> % Predicted	62.03 (22.94)	62.91 (22.59)	0.474
BODE Index	2.43 (2.44)	2.63 (2.38)	0.151
% Emphysema	11.27 (11.84)	9.39 (11.45)	0.003
Pack Years	53.05 (26.63)	47.57 (24.99)	<0.001
Airway Wall Thickness	1.17 (0.23)	1.00 (0.21)	<0.001
Exacerbation Frequency	0.37 (0.91)	0.54 (1.00)	0.002
Non-Hispanic White (%)	82	78	0.089
Current Smoker (%)	66	65	0.532
Diabetes (%)	17	14	0.197

COPD = Chronic Obstructive Pulmonary Disease

BMI = Body Mass Index

FEV<sub>1</sub> = Forced Expiratory Volume in 1 Second

BODE = Body mass index, Oairflow Obstruction, Dyspnea, and Exercise capacity

randomly split the data 50 times into train (75%) and test (25%) data sets keeping the proportions of males and females the same. Genes and proteins that were consistently selected across these splits were considered “stable” as these would be most likely to show consistent findings. Within each split, we performed supervised filtering using the training data by regressing exacerbation frequency on each of the genes and proteins retained after the unsupervised filtering. We used the `zeroinfl` function [Zeileis et al., 2008] where the current gene or protein was the only predictor in the count model and only an intercept for the zero model. Genes and proteins with an uncorrected p-value < 0.10 were included in the models. Because this supervised filtering was repeated for each split, a different set of variables could enter the models for each split of the data.

For existing methods, we fit the subgroup implementations described in Section 4.3 for CVR (using a Poisson family), SELPCCA-ZIP, Lasso (using a Poisson family), and Elastic Net (using a Poisson family). For HIP, we applied HIP (Grid) and HIP (Random) using the ZIP family and using the Poisson family [HIP (Grid)-Poisson and HIP (Random)-Poisson]. Additionally, we fit HIP using the ZIP family with an additional clinical data view that was not penalized [HIP (Grid)-ZIP+Clinical and HIP (Random)-ZIP+Clinical]. We used the training data to select tuning parameters and calculate training  $D^2$  and then used the test data to calculate a test  $D^2$ .

We defined the “stable” genes and proteins by ranking them based on the product of (a) the number of splits in which the variable was included in the  $N_{top}$  variables and (b) the number of splits in which the variable was included in the  $N_{top}$  variables divided by the number of splits in which the variable was entered into the models. The top 1% of genes and proteins for males and females based on this ranking were identified as the “stable” genes and proteins for each method.

To select tuning parameters, CVR, SELPCCA, Lasso, and Elastic Net used 10-fold cross-validation. For HIP, when we used the  $\lambda$  range (0, 2] used in simulations, the upper bound was consistently being selected, so we increased the range until this was not happening resulting in a range of (0, 15] for  $\lambda_G$  and  $\lambda_\xi$ . The best model was selected using  $eBIC_1$ . We also needed to specify  $K$ , the number of latent components for HIP and an equivalent parameter for CVR. The automatic approach specified in Butts et al. [2023] with a threshold of 0.20 on the concatenated data suggested  $K = 3$ . On the separate  $X^{d,s}$ , it suggested  $K = 3$  for the genes and  $K = 1$  for the proteins. Scree plots for the concatenated and separate data are in Supplemental Figure S11. We thus selected  $K = 3$  components for HIP and CVR. For HIP, we set  $N_{top} = 125$  genes and 50 proteins.

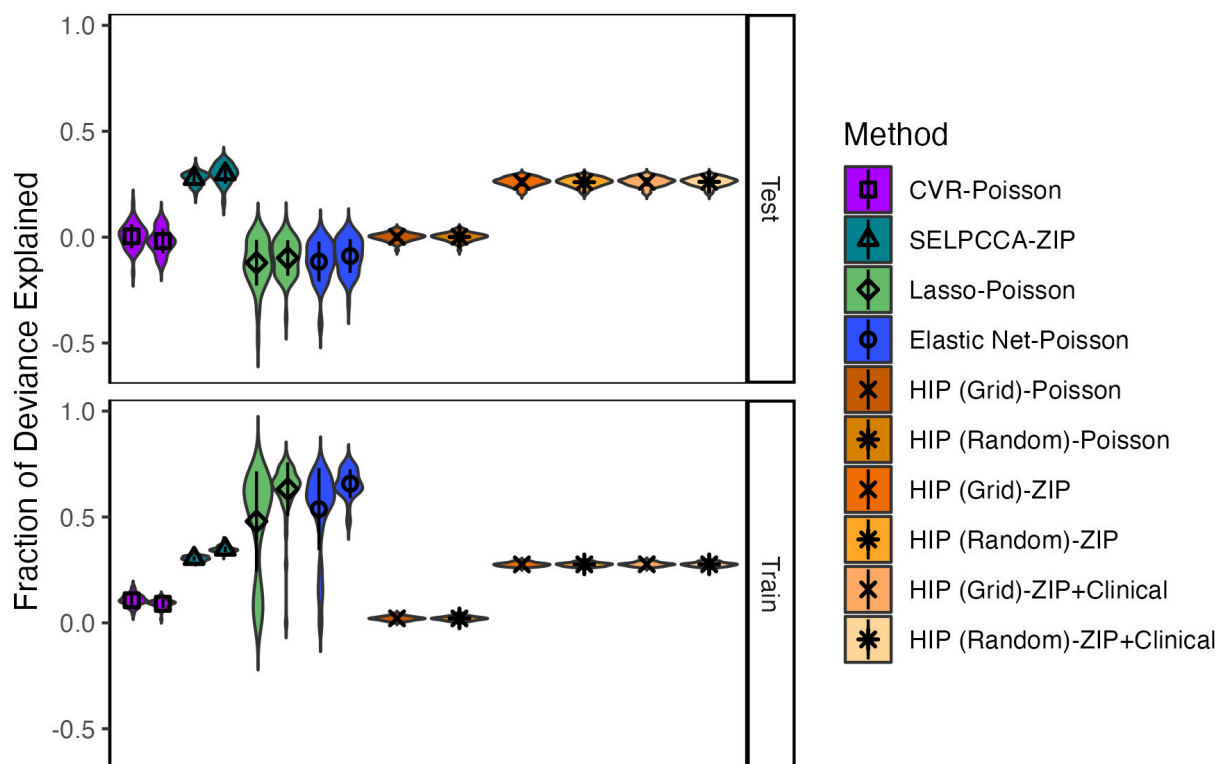
## 5.3 Results

### 5.3.1 Fraction of Deviance Explained and Computation Times

Figure 4 shows violin plots of the train and test fraction of deviance explained for the 50 Train/Test data splits. As expected, HIP (using ZIP model) and SELPCCA-ZIP, the two methods that account for the zero-inflated nature of the data, have the best predictive ability. The number of variables selected in the 50 Train/Test splits are summarized in Supplemental Table S1. Similarly, Supplemental Figure S12 shows a violin plot of the run times for each method. Of the methods performing integrative analysis, HIP (Random) regardless of family tended to have the fastest computation times, although SELPCCA-ZIP often had similar run times.



Figure 4: **Fraction of Deviance Explained Across 50 Data Splits of the COPDGene Data.** Violin plots display the distribution of fraction of deviance explained across the 50 data splits. For each of CVR, SELPCCA-ZIP, Lasso, and Elastic Net, there is a violin plot for each subgroup as comparator methods require separate models for each subgroup to allow for possible subgroup heterogeneity.



### 5.3.2 Selected Genes and Proteins

Supplemental Table S2 shows the number of “stable” genes and proteins common and specific to males and females identified by each method. Supplemental Figure S13 shows the overlap of “stable” genes and proteins selected for males and females by each method. There are few overlaps in the “stable” genes and proteins, but the overlaps that do occur tend to be in the methods that perform integrative analysis (i.e., HIP, CVR, and SELPCCA) suggesting integrative methods may result in more reproducible findings.

HIP (Random) and HIP (Grid) showed strong agreement in the “stable” genes and proteins (Supplemental Table S3) which also supports the use of the random search instead of the grid search. The “stable” genes selected by HIP (Random) for males and females and their average estimated weights are in Supplementary Tables S4 and S5 respectively. Analogous results for proteins are presented in Supplementary Table S6. The weights in these tables are averages of the estimated weights ( $L_2$  norm of rows in  $\hat{B}^{d,s}$ ) from the subset fit in the splits where the variable was included in the subset fit (i.e., the variable was in  $N_{top}$  for at least one subgroup).

The top gene for males was activating signal cointegrator 1 complex subunit (ASCC2). Wilson et al. [2020] looked for genes that were differentially expressed in COPD patients with and without cachexia (a loss of weight and muscle) and identified ASCC2 in a sample of 400 COPDGene Study participants and replicated the finding in a sample of 114 participants from the ECLIPSE Study; cachexia occurs more frequently in those with more advanced COPD. The top gene for females was dematin actin binding protein (DMTN). Lee et al. [2016] measured DNA methylation on 100 participants (60 with and 40 without COPD) from a Korean COPD Cohort and identified DMTN (also known as EPB49) as a differentially methylated region when comparing current smokers to never smokers; the authors also note this gene has been identified in previous epigenome-wide association studies of smoking. Thus this gene may be a candidate for future research to investigate the relationship with COPD specifically.

The top protein for males was SHC adaptor protein 1 (SHC1) (ranked fifth for females). Li et al. [2021] ranked candidate genes based on gene risk scores where a higher rank indicated a stronger relationship to COPD. The SHC1 gene was ranked third out of 200 candidate genes and had lower expression levels in patients with COPD compared to healthy controls. The top protein for females was amyloid beta precursor protein (APP) (ranked second for males). Almansa et al. [2012] compared gene expression levels of 12 patients with COPD requiring treatment in the ICU compared to 16 patients with COPD who were admitted to the hospital for treatment but did not require the ICU. They found that the patients admitted to the ICU showed higher expression levels of APP compared to patients who were not admitted to the ICU.

### 5.3.3 Pathway Analysis

We tested for overrepresentation of pathways in our “stable” proteins and genes for males and females using Ingenuity Pathway Analysis [Kramer et al., 2014]. Table 2 shows the top 10 canonical pathways for genes and proteins for males and females.

There were both common and subgroup-specific gene pathways for males and females. The top gene pathway for males was the CLEAR Signaling Pathway, and the top gene pathway for females was the STAT3 pathway. The STAT3 pathway is known to be involved in inflammatory responses to many diseases including COPD [Kiszałkiewicz et al., 2021]. The Iron homeostasis signaling pathway that was found in the AWT analysis in Butts et al. [2023] for both males and females was again present in the top gene pathways for males and females.

There was complete overlap in the top 10 protein pathways for males and females; this makes some sense because of the 20 stable proteins identified for males and females, 17 of them overlapped. For both males and females, the top pathway was the wound healing signaling pathway followed by PDGF signaling. The PDGF family includes PDGFA (platelet derived growth factor subunit A) and PDGFB (platelet derived growth factor subunit B) and is associated with wound healing; when PDGFs are found outside the context of wound healing, it seems to contribute to many diseases [Kardas et al., 2020]. Though these authors focus on asthma rather than COPD, they also state that PDGF is expressed in airway epithelial cells and PDGFB is expressed in inflamed airway tissue.

Table 2: Top 10 Canonical Pathways.

View	Subgroup	Canonical Pathway	Molecules	Unadjusted P-value
Genes	Males	CLEAR Signaling Pathway	ATP6VOC,IGF2R,PINK1,PPP2R5B	0.001
		STAT3 Pathway	IGF2R,IL1R1,PIMI	0.002
		IL-10 Signaling	BLVRB,IL1R2,PBX1	0.002
		Methylglyoxal Degradation I	HAGH	0.005
		Heme Degradation	BLVRB	0.007
		Histidine Degradation III	HAL	0.013
		$\gamma$ -glutamyl Cycle	ANPEP	0.020
		Iron homeostasis signaling pathway	ATP6VOC,SLC25A37	0.023
		Histidine Degradation VI	HAL	0.039
		Granulocyte Adhesion and Diapedesis	C5AR1,IL1R2	0.042
Proteins	Males	STAT3 Pathway	IGF2R,IL1R1,PIMI	0.001
		Iron homeostasis signaling pathway	ALAS2,ATP6VOC,SLC25A37	0.001
		Methylglyoxal Degradation I	HAGH	0.005
		Heme Degradation	BLVRB	0.006
		Tetrapyrrole Biosynthesis II	ALAS2	0.008
		Histidine Degradation III	HAL	0.012
		Heme Biosynthesis II	ALAS2	0.014
		Glycogen Degradation III	MGAM	0.020
		IL-10 Signaling	BLVRB,IL1R1	0.023
		Granulocyte Adhesion and Diapedesis	C5AR1,IL1R1	0.034
Proteins	Males	Wound Healing Signaling Pathway	CERT1,HBEGF,PDGFA,PDGFB,SHC1	<0.001
		PDGF Signaling	PDGFA,PDGFB,SHC1	<0.001
		PPAR Signaling	PDGFA,PDGFB,SHC1	<0.001
		Pulmonary Fibrosis Idiopathic Signaling Pathway	CERT1,PDGFA,PDGFB,THBS1	<0.001
		PAK Signaling	PDGFA,PDGFB,SHC1	<0.001
		Glioma Signaling	PDGFA,PDGFB,SHC1	<0.001
		DHCR24 Signaling Pathway	APP,PDGFA,PDGFB	<0.001
		Glioblastoma Multiforme Signaling	PDGFA,PDGFB,SHC1	<0.001
		Regulation of the Epithelial Mesenchymal Transition by Growth Factors Pathway	PDGFA,PDGFB,SHC1	<0.001
		Hepatic Fibrosis / Hepatic Stellate Cell Activation	CERT1,PDGFA,PDGFB	<0.001
Proteins	Females	Wound Healing Signaling Pathway	CERT1,HBEGF,PDGFA,PDGFB,SHC1	<0.001
		PDGF Signaling	PDGFA,PDGFB,SHC1	<0.001
		PPAR Signaling	PDGFA,PDGFB,SHC1	<0.001
		Pulmonary Fibrosis Idiopathic Signaling Pathway	CERT1,PDGFA,PDGFB,THBS1	<0.001
		PAK Signaling	PDGFA,PDGFB,SHC1	<0.001
		Glioma Signaling	PDGFA,PDGFB,SHC1	<0.001
		DHCR24 Signaling Pathway	APP,PDGFA,PDGFB	<0.001
		Glioblastoma Multiforme Signaling	PDGFA,PDGFB,SHC1	<0.001
		Regulation of the Epithelial Mesenchymal Transition by Growth Factors Pathway	PDGFA,PDGFB,SHC1	<0.001
		Hepatic Fibrosis / Hepatic Stellate Cell Activation	CERT1,PDGFA,PDGFB	<0.001

## 6 R Shiny Application

While HIP and its extension to additional outcomes has many research areas to which it could be applied (within and outside of human health), it is implemented in Python which may be a barrier to some researchers without a coding background. We introduce an R Shiny [Chang et al., 2023] application that provides a graphical interface to apply HIP to data that is either uploaded, simulated, or available within the application. In this section we provide a brief overview and highlights of the application. A detailed example of using the application is in the supplemental information. The application is accessible on shinyapps.io at [https://multi-viewlearn.shinyapps.io/HIP\\_ShinyApp/](https://multi-viewlearn.shinyapps.io/HIP_ShinyApp/).

The Shiny application has three tabs. The first tab, ‘About’, provides a brief overview of the method and related links (Figure 6). The second tab, ‘HIP’, is where the user will set-up the data and parameters for the method. We provide options for the user to upload their own data, simulate data (based on our simulation examples) and implement HIP on an example COVID-19 data (Figure 7). The third tab, ‘Results’, is where the user will submit the analysis and see results. This tab produces outputs of the model including prediction information and variable importance to help the user understand the results.

Once the ‘Run Analysis’ button has been clicked, a progress notification (Supplementary Figure S19) will appear in the lower right corner of the screen so the user knows the analysis has started. The user will know the analysis is complete when the progress notification disappears and the run time is displayed to the right of the ‘Run Analysis’ button. After the analysis is complete, the left column in the ‘Result Summary’ section will provide a button to download results, and the right column will display some basic information about the results for the user including the convergence status, the  $\lambda$  values used, the  $eBIC_0$  or other selection criterion value, the run time, and the applicable training prediction metric (Supplementary Figure S20). We also show prediction metric for the training data and the test data if they are available. If there are no test data available, a message will be printed for the user stating so. The prediction metric is the mean squared error for Gaussian outcomes, classification accuracy for multi-class outcomes, and fraction of deviance explained for Poisson and ZIP outcomes. The appropriate metric and formula are displayed in a gold box in the left column for users.

The weights from the estimated  $B^{d,s}$  matrices are displayed in two formats. The first is a variable importance plot that includes all variables that were included in the subset model fit (Supplementary Figure S22). The variables are ranked based on the weights within each view and subgroup. The second output is an interactive table with columns for the rank (within view and subgroup), variable, weight, view, and subgroup (Supplementary Figure S23). This table can be sorted by or filtered on any column so that the user can explore the results. Some possible options that could be of interest include selecting the top ranked variable(s) for each view and subgroup, selecting a specific variable to compare between subgroups, or selecting all results for a single view and subgroup (Supplementary Figures S24-S26).

In general, user inputs are in gray boxes, generated outputs have a white background, and information for the user is in gold boxes. Please refer to the supplementary material for detailed descriptions of HIP and an illustration of HIP on a publicly available data on COVID-19.

Figure 5: HIP Shiny Application Screens

Figure 6: 'About' Tab

One Stop MyU : For Students, Faculty, and Staff

About HIP Results

## Heterogeneity in Integration and Prediction

**Motivation:**  
Epidemiologic and genetic studies in chronic obstructive pulmonary disease (COPD) and many complex diseases suggest subgroup differences (e.g., by sex) in disease course and patient outcomes. We consider this from the standpoint of integrative analysis where we combine information from different views (e.g., genomics, proteomics, clinical data). Existing integrative analysis methods ignore the heterogeneity in subgroups, and methods accounting for subgroup heterogeneity do not model the association among the views.

**Description:**  
We propose HIP (Heterogeneity in Integration and Prediction), a statistical approach for joint association and prediction that leverages the strengths in each view to identify variables associated with an outcome of interest. HIP accounts for subgroup heterogeneity in multi-view data, ranks variables based on importance, can incorporate covariate adjustment, and is applicable to continuous, multi-class, Poisson, and Zero-Inflated Poisson (ZIP) outcomes. As such, this method has many potential scientific applications.

**Citing this work:**  
Please cite the following article(s) if you use this application in a publication.

- J. Butts, C. Wendt, R. Bowler, C. P. Hersh, Q. Long, L. Eberly, and S. E. Safo. Accounting for data heterogeneity in integrative analysis and prediction methods: An application to chronic obstructive pulmonary disease, 2021. [arXiv:2111.06962](https://arxiv.org/abs/2111.06962)

**Additional References:**

- [Chen & Chen \(2008\) Extended Bayesian Information Criteria for Model Selection with Large Model Spaces](#)

**Related Links:**

- [Python Code](#) - GitHub repository with underlying Python code
- [Multiview Dashboard](#) - Implements additional methods for analyzing multiview data

**Application Version:** 0.1.4

Figure 7: Input Data - COVID-19 Example

## Input Data

**Select the source of your data:**

Upload my own data

Simulate data

Covid data

Click 'Submit Data' once data details have been entered.

**Outcome Variable**

HFD45

**Subgroup Variable**

DiseaseStatus

**Type of Outcome**

ZIP

**Description of Variables**

- HFD45** : Number of hospital free days out of the 45 days enrolled in the study; A zero indicates the patient was either still in the hospital or died.
- VentFreeDays** : Number of ventilator free days out of the 45 days enrolled in the study
- ICU.Status** : Intensive Care Unit status
- MechVentStatus** : Mechanical ventilation status
- DiseaseStatus** : COVID-19 infection status
- Sex** : Biological sex

[Overmeyer et al. \(2021\) \[Source of Data\]](#)  
[Lipman et al. \(2022\) \[Preprocessing of Data\]](#)

## 7 Conclusion

In this paper, we have extended HIP as proposed in Butts et al. [2023] to accommodate multi-class, Poisson, and zero-inflated Poisson (ZIP) outcomes allowing researchers to investigate additional clinically relevant outcomes in an integrative analysis framework that also accounts for subgroup heterogeneity. We retain the benefits of a joint association and prediction method for data integration to select clinically meaningful subgroup-specific and common features and the ability to include clinical covariates. In simulations, HIP demonstrated improved variable selection abilities for binary, Poisson, and ZIP outcomes compared to existing methods. While all methods showed similar classification accuracy in the binary outcome simulations, HIP showed small improvements in  $D^2$  in the Poisson outcome simulations and substantial improvements in  $D^2$  in the ZIP outcome simulations. When applied to data from the COPDGene Study, we were able to identify common and subgroup-specific genes and proteins associated with exacerbation frequency; previous literature has identified at least some of these as being related to COPD.

The R Shiny Application developed here provides a user-friendly interface to apply HIP to any data with multiple data views, measured on pre-specified subgroups, being used to predict an outcome. In the first tab, the application introduces HIP and describes why HIP may be a desirable method to consider for analyzing a multi-view data set with potential subgroup heterogeneity. In the second tab, the application guides the user through inputting data, selecting an appropriate  $K$ , and setting parameters for running HIP. Finally, the third tab produces outputs of the model including prediction information and variable importance to help the user understand the results.

There are still some limitations to HIP requiring further research. As in the originally proposed HIP [Butts et al., 2023],  $N_{top}$ , the number of variables to keep for each view, must be specified. In simulations, we know the true value of  $N_{top}$ , but we cannot know the true value in applications to real data. Sensitivity analyses could help investigate the performance when values other than the true value are specified. Additionally, the inclusion of clinical covariates in the COPDGene application did not improve predictive abilities on the test data. The reason for this is unclear and could be for multiple reasons. One possibility is the variables in the clinical view do not explain additional variation in the outcome beyond the genes and proteins. Another possibility is that the large difference in the number of variables in this view compared to the other views affects the estimation. Despite these limitations, this extension to HIP allows researchers to explore a wide variety of new questions by considering multi-class, Poisson, or ZIP outcomes that are clinically meaningful.

## Supporting information

Additional supporting information may be found in the online version of the article at the publisher’s website. The Python code for implementing HIP is publicly available on GitHub at <https://github.com/lasandrall/HIP>. An R-package for HIP would also be made available at this same link.

## Acknowledgements

This work was supported NIGMS grant 1R35GM142695, NHLBI grants U01 HL089897 and U01 HL089856 and by NIH contract 75N92023D00011. The COPDGene study (NCT00608764) is also supported by the COPD Foundation through contributions made to an Industry Advisory Committee that has included AstraZeneca, Bayer Pharmaceuticals, Boehringer-Ingelheim, Genentech, GlaxoSmithKline, Novartis, Pfizer, and Sunovion.

## References

- Joan B Soriano, Parkes J Kendrick, Katherine R Paulson, Vinay Gupta, Elissa M Abrams, et al. Prevalence and attributable health burden of chronic respiratory diseases, 1990–2017: a systematic analysis for the global burden of disease study 2017. *The Lancet Respiratory Medicine*, 8(6):585–596, June 2020. ISSN 2213-2600. doi:10.1016/S2213-2600(20)30105-3. URL [https://doi.org/10.1016/S2213-2600\(20\)30105-3](https://doi.org/10.1016/S2213-2600(20)30105-3).
- Alvar Agustí, Bartolome R Celli, Gerard J Criner, David Halpin, Antonio Anzueto, Peter Barnes, Jean Bourbeau, MeiLan K Han, Fernando J Martinez, Maria Montes de Oca, et al. Global initiative for chronic obstructive lung disease 2023 report: Gold executive summary. *American journal of respiratory and critical care medicine*, 207(7): 819–837, 2023.
- Edwin K. Silverman. Genetics of copd. *Annual Review of Physiology*, 82(1):413–431, 2020. doi:10.1146/annurev-physiol-021317-121224. URL <https://doi.org/10.1146/annurev-physiol-021317-121224>. PMID: 31730394.

- Megan Hardin and Edwin K Silverman. Chronic obstructive pulmonary disease genetics: a review of the past and a look into the future. Chronic Obstructive Pulmonary Diseases: Journal of the COPD Foundation, 1(1):33, 2014.
- Guoping Hu, Yumin Zhou, Jia Tian, Weimin Yao, Jianguo Li, Bing Li, and Pixin Ran. Risk of copd from exposure to biomass smoke: a meta-analysis. Chest, 138(1):20–31, 2010.
- KF Chung and IM Adcock. Multifaceted mechanisms in copd: inflammation, immunity, and tissue repair and destruction. European Respiratory Journal, 31(6):1334–1356, 2008.
- Wen Qi Gan, SF Paul Man, Dirkje S Postma, Patricia Camp, and Don D Sin. Female smokers beyond the perimenopausal period are at increased risk of chronic obstructive pulmonary disease: a systematic review and meta-analysis. Respiratory research, 7(1):1–9, 2006.
- Yu-II Kim, Joyce Schroeder, David Lynch, John Newell, Barry Make, Adam Friedlander, Raúl San José Estépar, Nicola A Hanania, George Washko, James R Murphy, et al. Gender differences of airway dimensions in anatomically matched sites on ct in smokers. COPD: Journal of Chronic Obstructive Pulmonary Disease, 8(4):285–292, 2011.
- E Prescott, AM Bjerg, PK Andersen, P Lange, and J Vestbo. Gender difference in smoking effects on lung function and risk of hospitalization for copd: results from a danish longitudinal population study. European Respiratory Journal, 10(4):822–827, 1997.
- Elizabeth A Regan, John E Hokanson, James R Murphy, Barry Make, David A Lynch, Terri H Beaty, Douglas Curran-Everett, Edwin K Silverman, and James D Crapo. Genetic epidemiology of copd (copdgene) study design. COPD: Journal of Chronic Obstructive Pulmonary Disease, 7(1):32–43, 2011.
- Jessica Butts, Christine Wendt, Russel P. Bowler, Craig P. Hersh, Qi Long, Lynn Eberly, and Sandra E. Safo. Accounting for data heterogeneity in integrative analysis and prediction methods: An application to chronic obstructive pulmonary disease. 2023. URL <https://arxiv.org/abs/2111.06962>. Under review.
- Ann Evenson. Management of copd exacerbations. American Family Physician, 81(5), 8 2010. PMID: 20187597.
- Bartolome Celli, Jørgen Vestbo, Christine R. Jenkins, Paul W. Jones, Gary T. Ferguson, Peter M. A. Calverley, Julie C. Yates, Julie A. Anderson, Lisa R. Willits, and Robert A. Wise. Sex differences in mortality and clinical expressions of patients with chronic obstructive pulmonary disease. American Journal of Respiratory and Critical Care Medicine, 183(3):317–322, 2011. doi:10.1164/rccm.201004-0665OC. URL <https://doi.org/10.1164/rccm.201004-0665OC>. PMID: 20813884.
- Hui Zou and Trevor Hastie. Regularization and variable selection via the elastic net. Journal of the Royal Statistical Society, Series B, 67:301–320, 2005.
- Robert Tibshirani. Regression shrinkage and selection via the lasso. JOURNAL OF THE ROYAL STATISTICAL SOCIETY, SERIES B, 58:267–288, 1994.
- Jerome Friedman, Trevor Hastie, and Robert Tibshirani. Regularization paths for generalized linear models via coordinate descent. Journal of Statistical Software, 33(1):1–22, 2010. URL <http://www.jstatsoft.org/v33/i01/>.
- Chongliang Luo, Jin Liu, Dipak K Dey, and Kun Chen. Canonical variate regression. Biostatistics, 17(3):468–483, 2016.
- Sandra E. Safo, Eun Jeong Min, and Lillian Haine. Sparse linear discriminant analysis for multiview structured data. Biometrics, n/a(n/a), 2021. doi:<https://doi.org/10.1111/biom.13458>. URL <https://onlinelibrary.wiley.com/doi/abs/10.1111/biom.13458>.
- Sandra E. Safo, Jeongyoun Ahn, Yongho Jeon, and Sungkyu Jung. Sparse generalized eigenvalue problem with application to canonical correlation analysis for integrative analysis of methylation and gene expression data. Biometrics, 74(4):1362–1371, 2018. doi:<https://doi.org/10.1111/biom.12886>. URL <https://onlinelibrary.wiley.com/doi/abs/10.1111/biom.12886>.
- Frank Dondelinger, Sach Mukherjee, and The Alzheimer’s Disease Neuroimaging Initiative. The joint lasso: high-dimensional regression for group structured data. Biostatistics, 21(2):219–235, 2018. ISSN 1465-4644. doi:10.1093/biostatistics/kxy035. URL <https://doi.org/10.1093/biostatistics/kxy035>.
- Winston Chang, Joe Cheng, JJ Allaire, Carson Sievert, Barret Schloerke, Yihui Xie, Jeff Allen, Jonathan McPherson, Alan Dipert, and Barbara Borges. shiny: Web Application Framework for R, 2023. URL <https://CRAN.R-project.org/package=shiny>. R package version 1.7.4.1.
- Quefeng Li, Sijian Wang, Chiang-Ching Huang, Menggang Yu, and Jun Shao. Meta-analysis based variable selection for gene expression data. Biometrics, 70(4):872–880, 2014.
- Diane Lambert. Zero-inflated poisson regression, with an application to defects in manufacturing. Technometrics, 34(1):1–14, 1992. ISSN 00401706. URL <http://www.jstor.org/stable/1269547>.

- Adam Paszke, Sam Gross, Francisco Massa, Adam Lerer, James Bradbury, Gregory Chanan, Trevor Killeen, Zeming Lin, Natalia Gimelshein, Luca Antiga, Alban Desmaison, Andreas Kopf, Edward Yang, Zachary DeVito, Martin Raison, Alykhan Tejani, Sasank Chilamkurthy, Benoit Steiner, Lu Fang, Junjie Bai, and Soumith Chintala. Pytorch: An imperative style, high-performance deep learning library. In H. Wallach, H. Larochelle, A. Beygelzimer, F. d'Alché-Buc, E. Fox, and R. Garnett, editors, *Advances in Neural Information Processing Systems 32*, pages 8024–8035. Curran Associates, Inc., 2019. URL <http://papers.neurips.cc/paper/9015-pytorch-an-imperative-style-high-performance-deep-learning-library.pdf>.
- Amir Beck and Marc Teboulle. A fast iterative shrinkage-thresholding algorithm for linear inverse problems. *SIAM J. Img. Sci.*, 2(1):183–202, March 2009. doi:10.1137/080716542. URL <https://doi.org/10.1137/080716542>.
- John Duchi, Elad Hazan, and Yoram Singer. Adaptive subgradient methods for online learning and stochastic optimization. *Journal of Machine Learning Research*, 12(61):2121–2159, 2011. URL <http://jmlr.org/papers/v12/duchi11a.html>.
- James Bergstra and Yoshua Bengio. Random search for hyper-parameter optimization. *Journal of Machine Learning Research*, 13(Feb):281–305, 2012.
- Jiahua Chen and Zehua Chen. Extended bayesian information criteria for model selection with large model spaces. *Biometrika*, 95:759–771, 2008. doi:10.1093/biomet/asn034.
- Chongliang Luo and Kun Chen. CVR: Canonical Variate Regression, 2017. URL <https://CRAN.R-project.org/package=CVR>. R package version 0.1.1.
- Sandra E. Safo and Elise F. Palzer. *mvlearnR: Multiview Learning Methods in R*, 2022. URL [https://multi-viewlearn.shinyapps.io/MultiView\\_Modeling/](https://multi-viewlearn.shinyapps.io/MultiView_Modeling/). <https://github.com/lasandrall/mvlearnR>.
- Achim Zeileis, Christian Kleiber, and Simon Jackman. Regression models for count data in R. *Journal of Statistical Software*, 27(8), 2008. URL <http://www.jstatsoft.org/v27/i08/>.
- Simon Jackman. *psc1: Classes and Methods for R Developed in the Political Science Computational Laboratory*. United States Studies Centre, University of Sydney, Sydney, New South Wales, Australia, 2020. URL <https://github.com/atahk/psc1/>. R package version 1.5.5.1.
- Trevor Hastie, Robert Tibshirani, and Martin Wainwright. *Statistical Learning with Sparsity: The Lasso and Generalizations*. CRC Press, 2016.
- Ava C. Wilson, Preeti L. Kumar, Sool Lee, Margaret M. Parker, Itika Arora, Jarrett D. Morrow, Emiel F. M. Wouters, Richard Casaburi, Stephen I. Rennard, David A. Lomas, Alvar Agusti, Ruth Tal-Singer, Mark T. Dransfield, J. Michael Wells, Surya P. Bhatt, George Washko, Victor J. Thannickal, Hemant K. Tiwari, Craig P. Hersh, Peter J. Castaldi, Edwin K. Silverman, and Merry-Lynn N. McDonald. Heme metabolism genes downregulated in copd cachexia. *Respiratory Research*, 21(1):100, 12 2020. ISSN 1465-993X. doi:10.1186/s12931-020-01336-w.
- Mi Kyeong Lee, Yoonki Hong, Sun-Young Kim, Stephanie J. London, and Woo Jin Kim. Dna methylation and smoking in korean adults: epigenome-wide association study. *Clinical Epigenetics*, 8(1):103, 12 2016. ISSN 1868-7075, 1868-7083. doi:10.1186/s13148-016-0266-6.
- Wan Li, Yihua Zhang, Yahui Wang, Zherou Rong, Chenyu Liu, Hui Miao, Hongwei Chen, Yuehan He, Weiming He, and Lina Chen. Candidate gene prioritization for chronic obstructive pulmonary disease using expression information in protein–protein interaction networks. *BMC Pulmonary Medicine*, 21(1):280, 12 2021. ISSN 1471-2466. doi:10.1186/s12890-021-01646-9.
- Raquel Almansa, Lorenzo Socias, Monica Sanchez-Garcia, Ignacio Martín-Loeches, Milagros Del Olmo, David Andaluz-Ojeda, Felipe Bobillo, Lucia Rico, Agueda Herrero, Vicente Roig, C Alicia San-Jose, Sara Rosich, Julia Barbado, Carlos Disdier, Raúl Ortiz De Lejarazu, Maria C Gallegos, Victoria Fernandez, and Jesus F Bermejo-Martin. Critical copd respiratory illness is linked to increased transcriptomic activity of neutrophil proteases genes. *BMC Research Notes*, 5(1):401, 12 2012. ISSN 1756-0500. doi:10.1186/1756-0500-5-401.
- Andreas Kramer, Jeff Green, Jack Pollard Jr., and Stuart Tugendreich. Causal analysis approaches in ingenuity pathway analysis. *Bioinformatics*, 30(4):523–530, 2014. doi:10.1093/bioinformatics/btt703. URL <https://doi.org/10.1093/bioinformatics/btt703>.
- J. M. Kiszalkiewicz, S. Majewski, W. J. Piotrowski, P. Górski, D. Pastuszek-Lewandoska, M. Migdalska-Sek, and E. Brzezińska-Lasota. Evaluation of selected il6/stat3 pathway molecules and mirna expression in chronic obstructive pulmonary disease. *Scientific Reports*, 11(1):22756, 11 2021. ISSN 2045-2322. doi:10.1038/s41598-021-01950-8.
- Grzegorz Kardas, Agnieszka Daszyńska-Kardas, Mateusz Marynowski, Oliwia Brzakalska, Piotr Kuna, and Michał Panek. Role of platelet-derived growth factor (pdgf) in asthma as an immunoregulatory factor mediating airway remodeling and possible pharmacological target. *Frontiers in Pharmacology*, 11:47, 2 2020. ISSN 1663-9812. doi:10.3389/fphar.2020.00047.



---

# SUPPLEMENTARY MATERIAL TO EXTENSIONS OF HETEROGENEITY IN INTEGRATION AND PREDICTION (HIP) WITH R SHINY APPLICATION

---

A PREPRINT

**Jessica Butts, PhD**  
Division of Biostatistics  
University of Minnesota Twin Cities


**Christine Wendt, MD**  
Division of Pulmonary, Allergy and Critical Care  
University of Minnesota Twin Cities

**Russel Bowler, MD, PhD**  
Division of Pulmonary, Critical Care and Sleep Medicine  
Department of Medicine  
National Jewish Health

**Craig P. Hersh, MD**  
Channing Division of Network Medicine  
Brigham and Women's Hospital  
Harvard Medical School

**Qi Long, PhD**  
Department of Biostatistics, Epidemiology and Informatics  
Perelman School of Medicine  
University of Pennsylvania

**Lynn Eberly, PhD**  
Division of Biostatistics  
University of Minnesota Twin Cities

 **Sandra E. Safo\***  
Division of Biostatistics  
University of Minnesota Twin Cities  
ssafo@umn.edu

October 13, 2023

## 1 Additional Displays of Simulation Results

This section includes all simulation results for the binary and Poisson outcomes. This includes evaluations of performance in terms of variable selection and predictive ability and computation times. The computation times for the ZIP simulations are also presented.

---

\*Corresponding Author: Sandra Safo, [www.sandraesafo.com](http://www.sandraesafo.com)

Figure S1: **Results for Binary Outcome, Full Overlap Scenario.** The first row corresponds to the low dimension ( $p_1 = 300, p_2 = 350$ ) and the second to the high dimension ( $p_1 = 2000, p_2 = 3000$ ). For all settings,  $n_1 = 250$  and  $n_2 = 260$ . The right column is classification accuracy, so a higher value indicates better performance. Results are mean  $\pm$  one standard deviation summarized across 20 generated data sets.

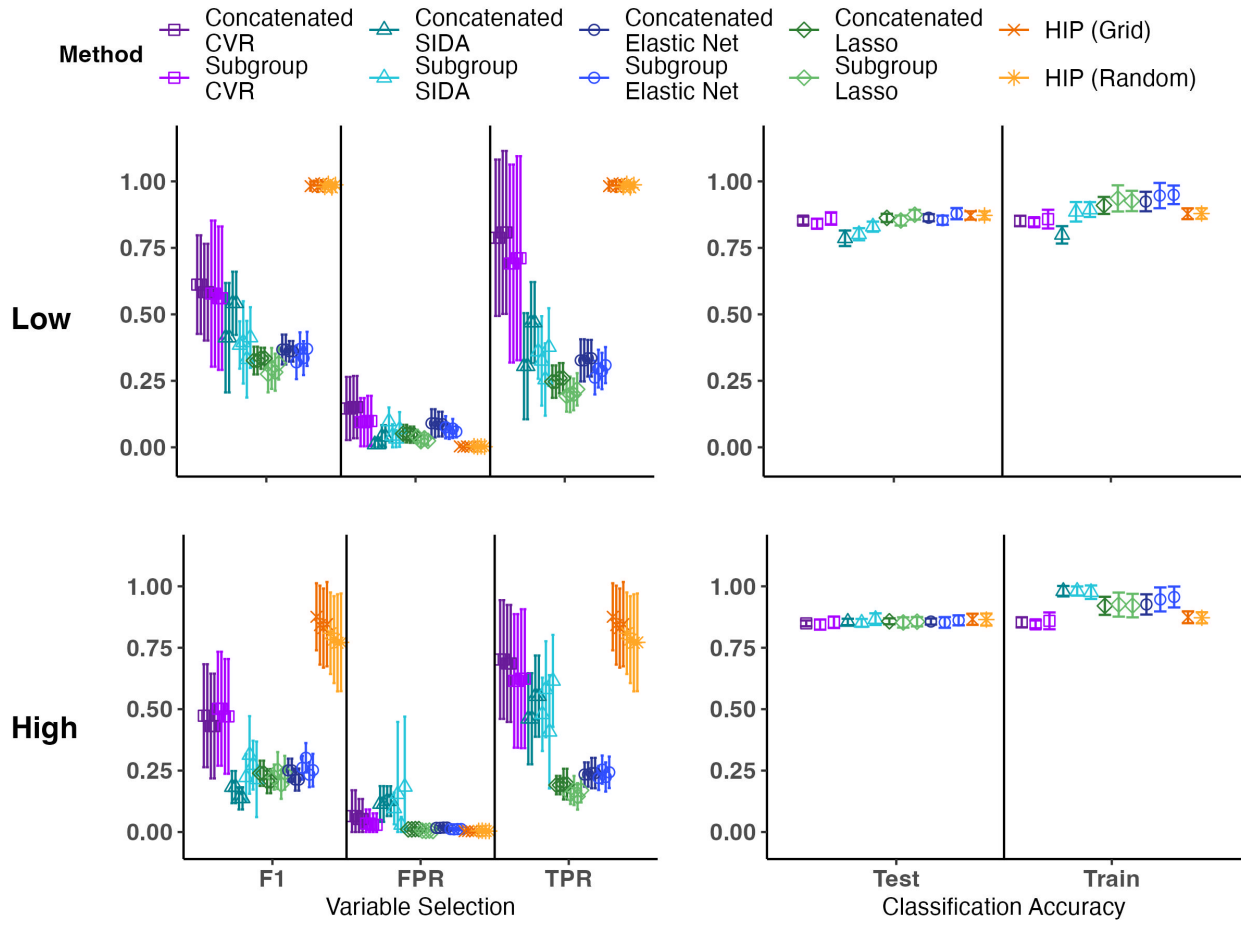


Figure S2: **Computation Time for Binary Outcome, Full Overlap Scenario.** HIP (Random) has the fastest computation time of methods that perform integration or account for subgroup heterogeneity. In the high dimension setting, the computation time for CVR increases dramatically. Results are mean  $\pm$  one standard deviation summarized across 20 generated data sets.

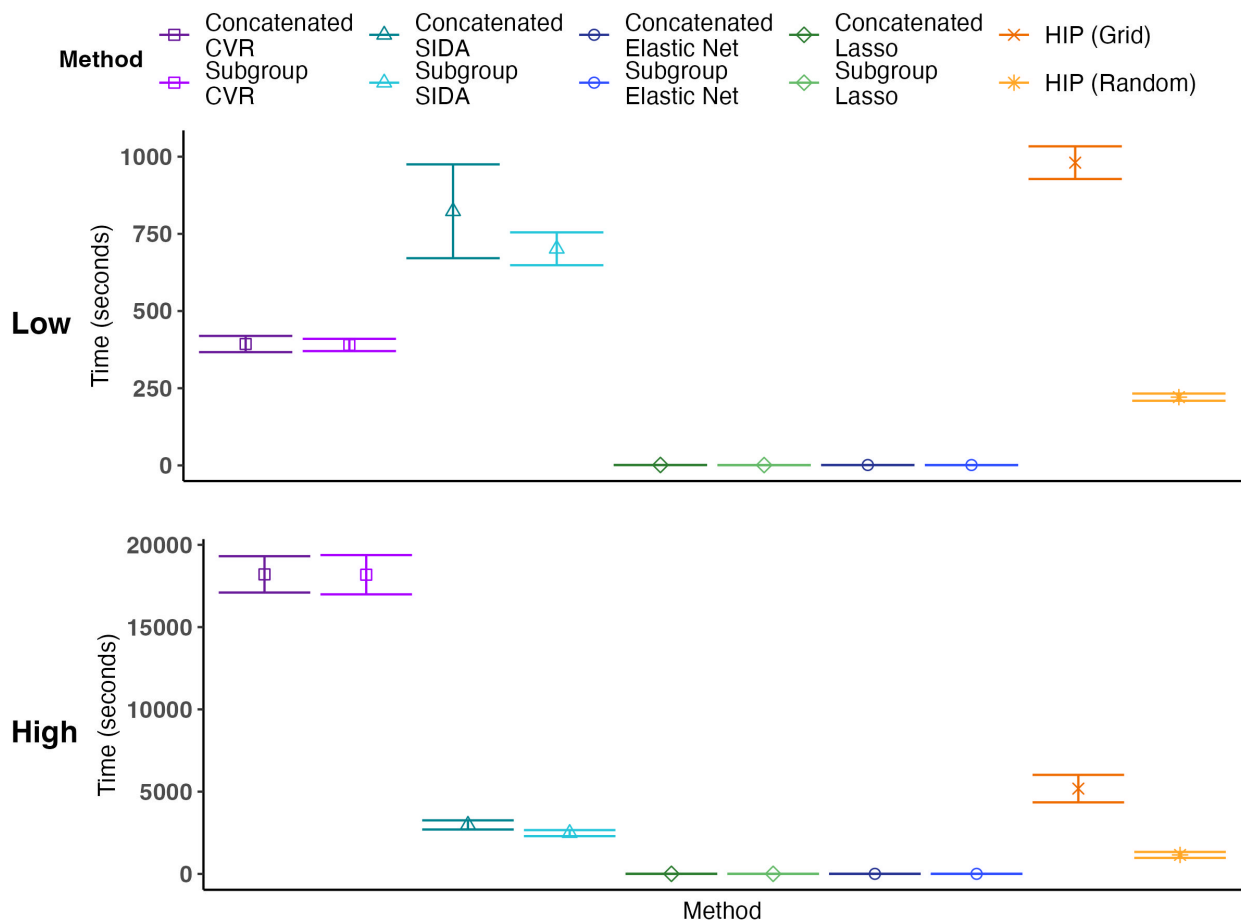


Figure S3: **Results for Binary Outcome, Partial Overlap Scenario.** The first row corresponds to the low dimension ( $p_1 = 300, p_2 = 350$ ) and the second to the high dimension ( $p_1 = 2000, p_2 = 3000$ ). For all settings,  $n_1 = 250$  and  $n_2 = 260$ . The right column is classification accuracy, so a higher value indicates better performance. Results are mean  $\pm$  one standard deviation summarized across 20 generated data sets.

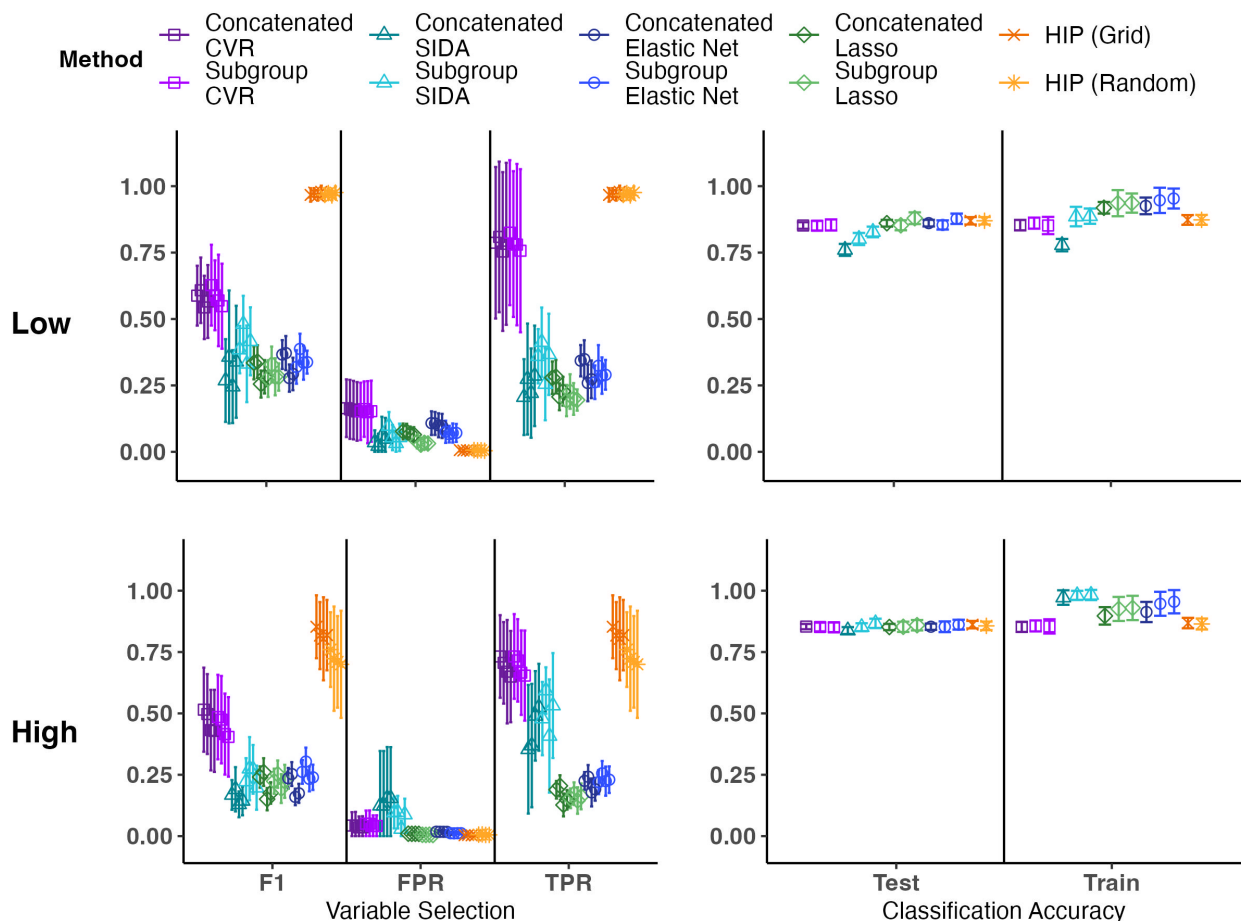


Figure S4: **Computation Time for Binary Outcome, Partial Overlap Scenario.** HIP (Random) has the fastest computation time of methods that perform integration or account for subgroup heterogeneity. In the high dimension setting, the computation time for CVR increases dramatically. Results are mean  $\pm$  one standard deviation summarized across 20 generated data sets.

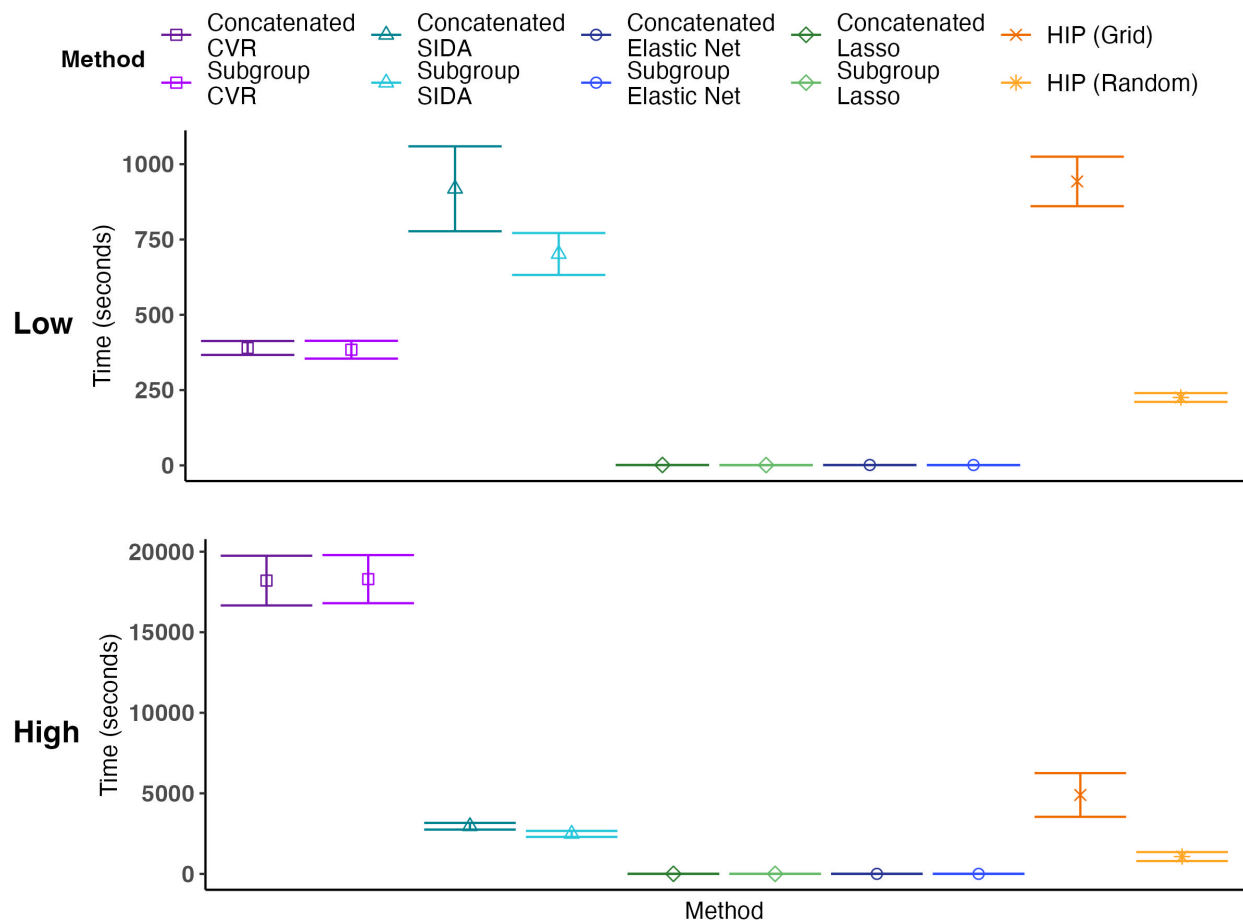


Figure S5: **Results for Poisson Outcome, Full Overlap Scenario.** The first row corresponds to the low dimension ( $p_1 = 300, p_2 = 350$ ) and the second to the high dimension ( $p_1 = 2000, p_2 = 3000$ ). For all settings,  $n_1 = 250$  and  $n_2 = 260$ . The right column is fraction of deviance explained ( $D^2$ ), so a higher value indicates better performance. Results are mean  $\pm$  one standard deviation summarized across 20 generated data sets.

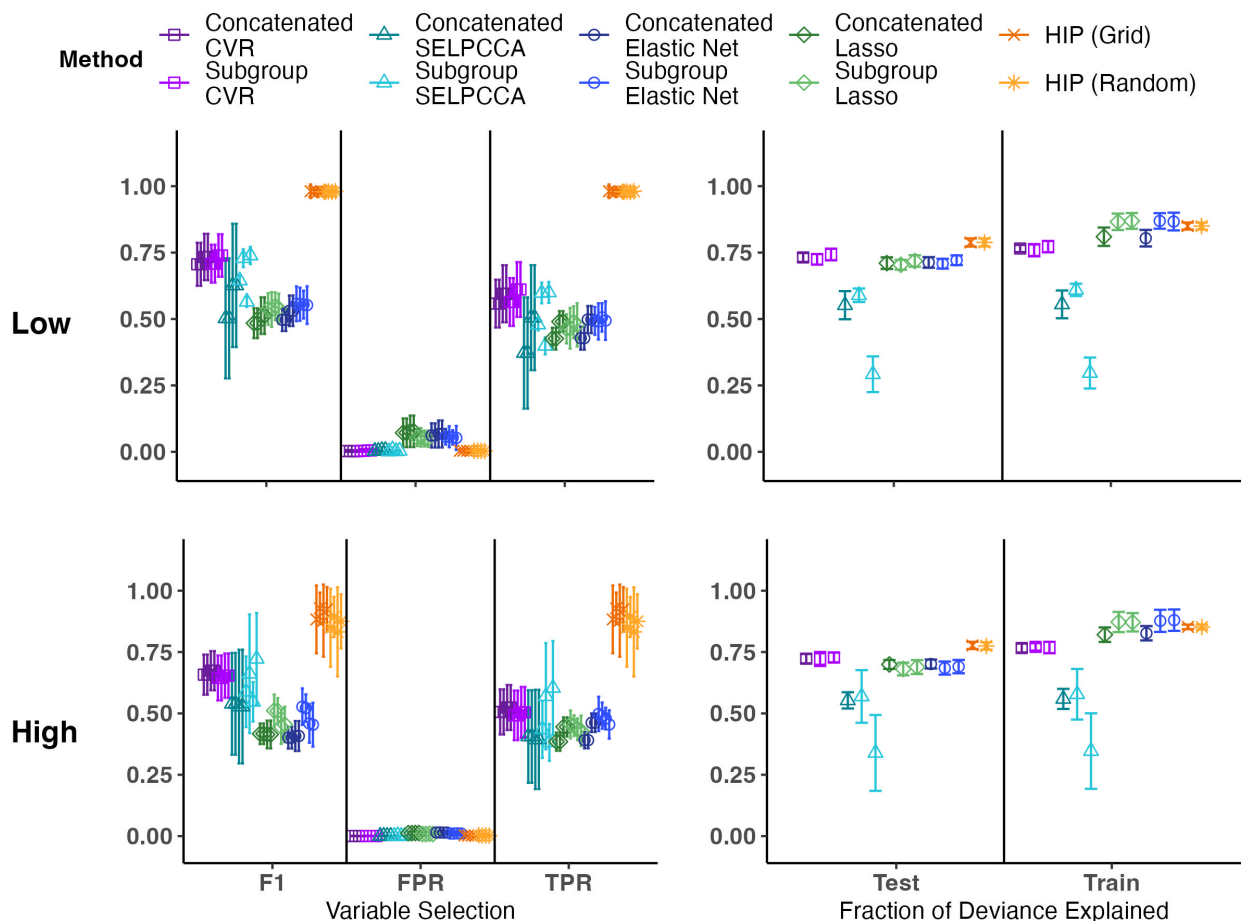


Figure S6: **Computation Time for Poisson Outcome, Full Overlap Scenario.** HIP (Random) has the fastest computation time of methods that perform integration or account for subgroup heterogeneity. In the high dimension setting, the computation time for CVR increases dramatically. Results are mean  $\pm$  one standard deviation summarized across 20 generated data sets.

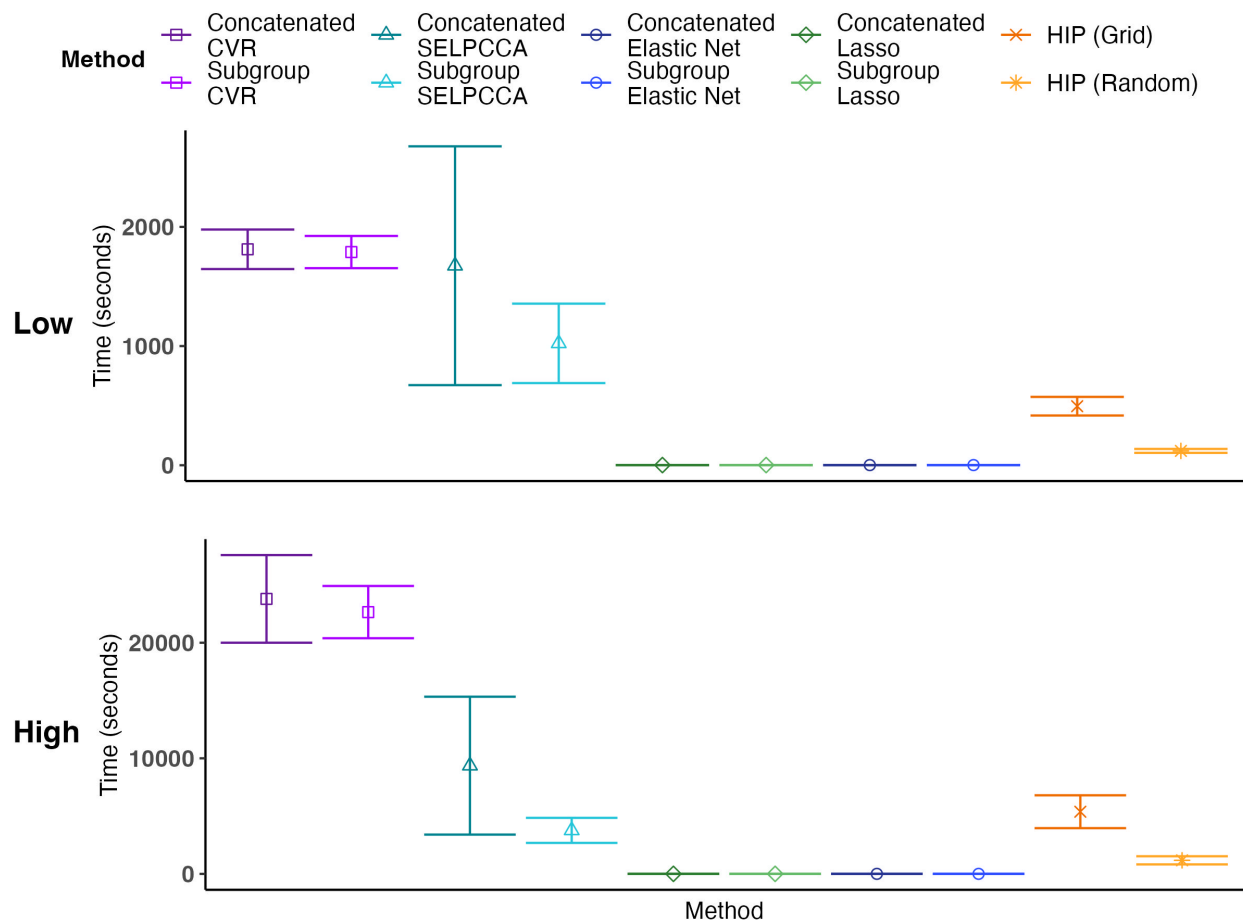


Figure S7: **Results for Poisson Outcome, Partial Overlap Scenario.** The first row corresponds to the low dimension ( $p_1 = 300, p_2 = 350$ ) and the second to the high dimension ( $p_1 = 2000, p_2 = 3000$ ). For all settings,  $n_1 = 250$  and  $n_2 = 260$ . The right column is fraction of deviance explained ( $D^2$ ), so a higher value indicates better performance. Results are mean  $\pm$  one standard deviation summarized across 20 generated data sets.

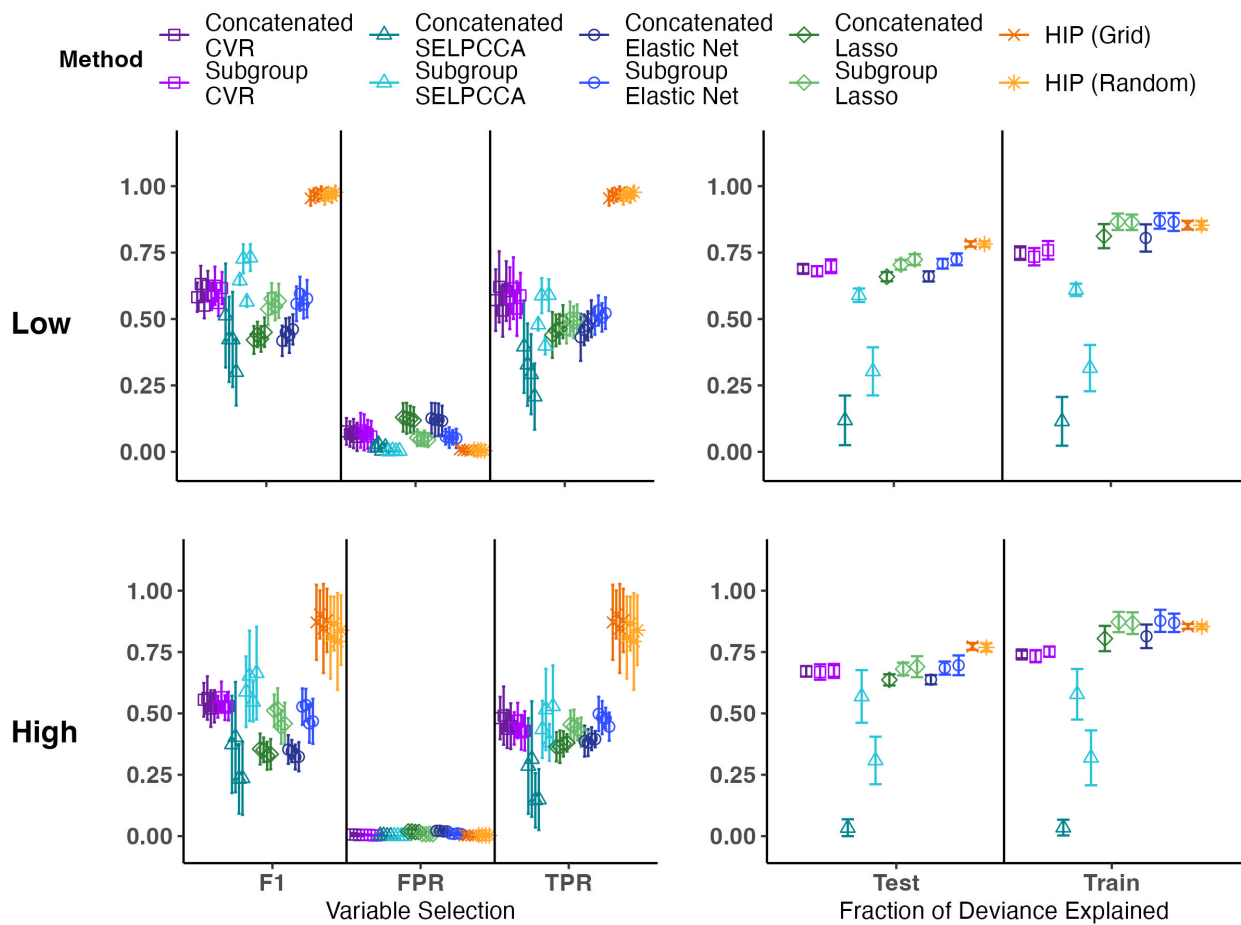




Figure S8: **Computation Time for Poisson Outcome, Partial Overlap Scenario.** HIP (Random) has the fastest computation time of methods that perform integration or account for subgroup heterogeneity. In the high dimension setting, the computation time for CVR increases dramatically. Results are mean  $\pm$  one standard deviation summarized across 20 generated data sets.

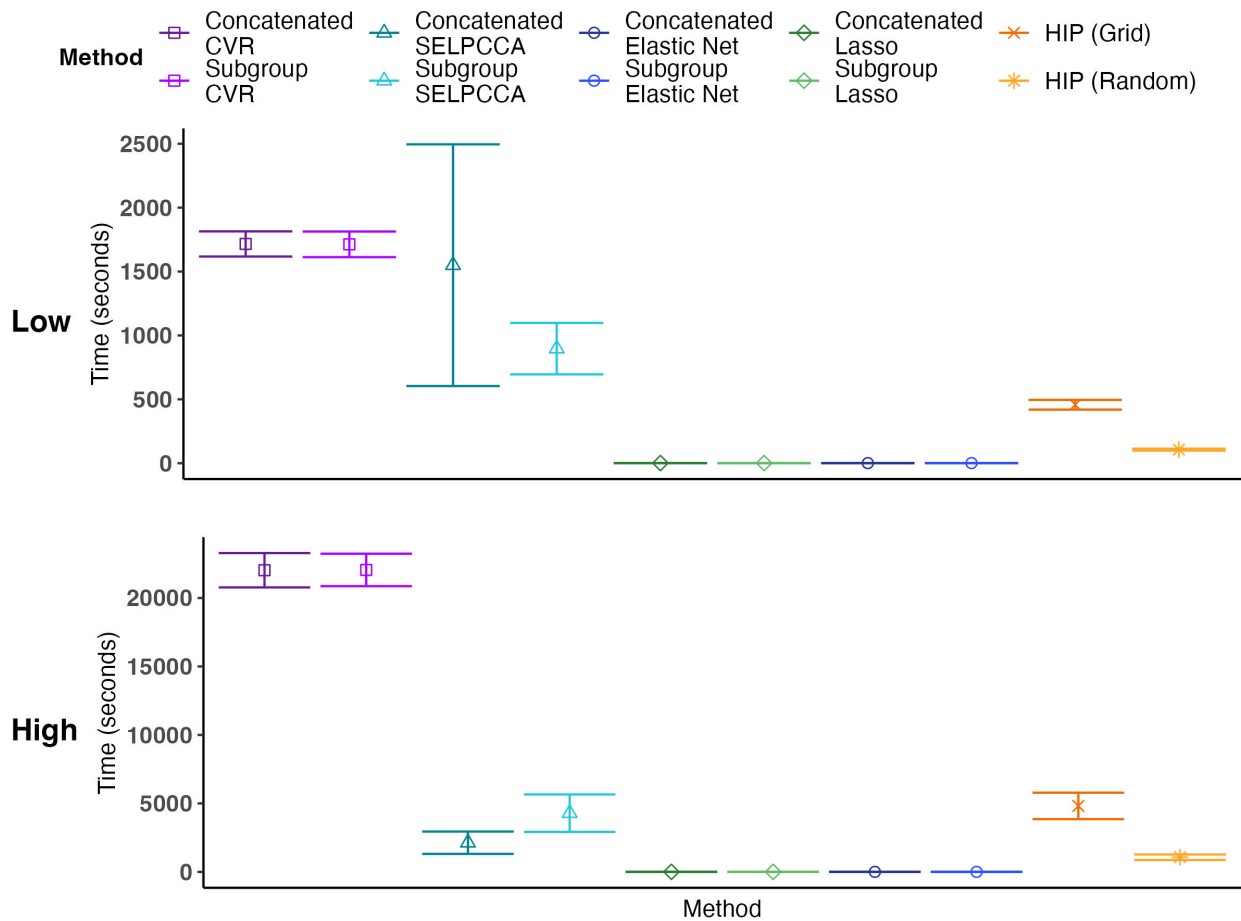


Figure S9: **Computation Time for ZIP Outcome, Full Overlap Scenario.** HIP (Random) has the fastest computation time of methods that perform integration or account for subgroup heterogeneity. In the high dimension setting, the computation time for CVR increases dramatically. Results are mean  $\pm$  one standard deviation summarized across 20 generated data sets.

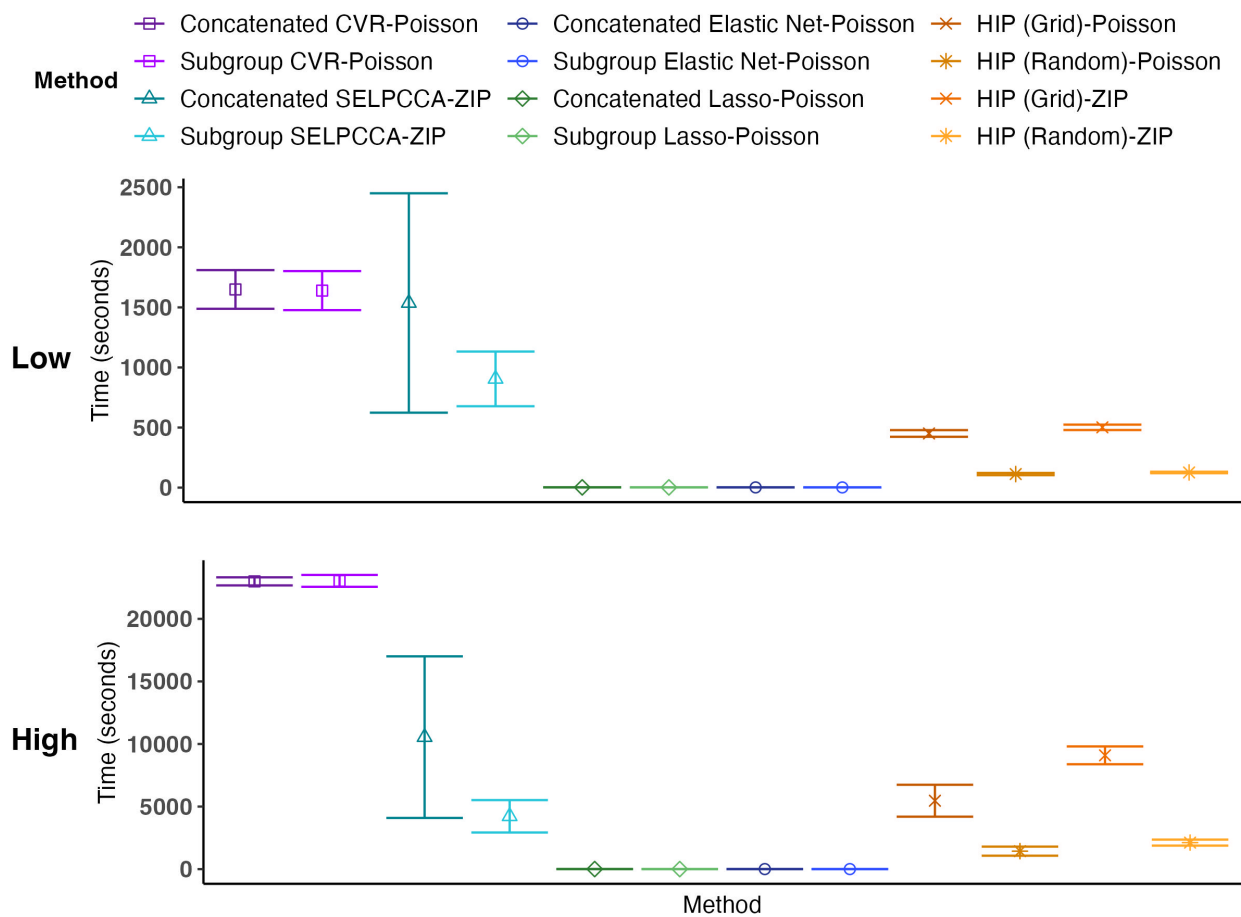
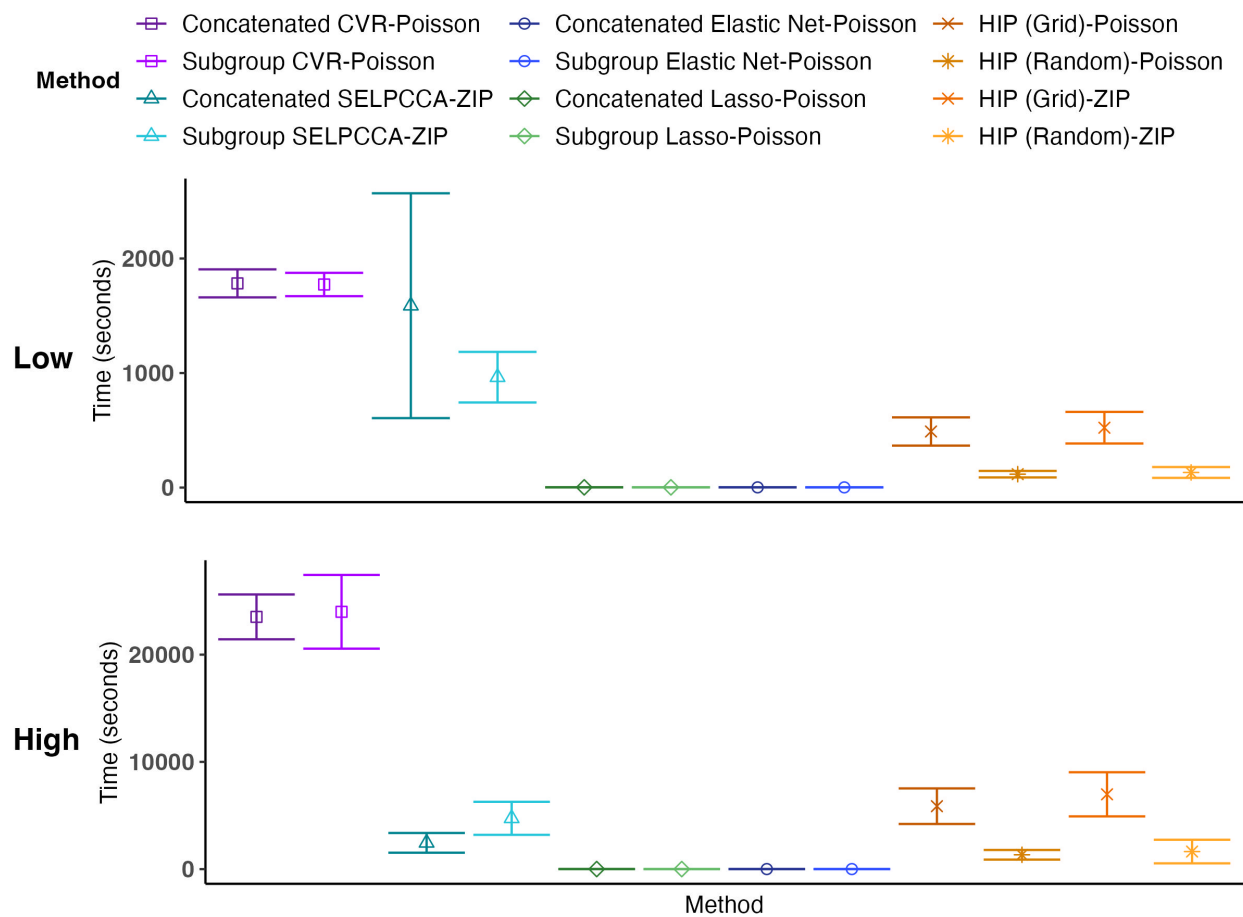


Figure S10: **Computation Time for ZIP Outcome, Partial Overlap Scenario.** HIP (Random) has the fastest computation time of methods that perform integration or account for subgroup heterogeneity. In the high dimension setting, the computation time for CVR increases dramatically. Results are mean  $\pm$  one standard deviation summarized across 20 generated data sets.



## 2 Additional Displays of COPD Application Results

This section includes additional displays of the results from the application to the COPDGene Study data using exacerbation frequency as the outcome.

Figure S11: **Scree Plot for COPDGene Data.** The automatic selection approach with a threshold of 0.20 suggested  $K = 3$  for the concatenated data, and for view and sub-group specific data views, it suggested  $K = 3$  for the gene data and  $K = 1$  for the protein data.

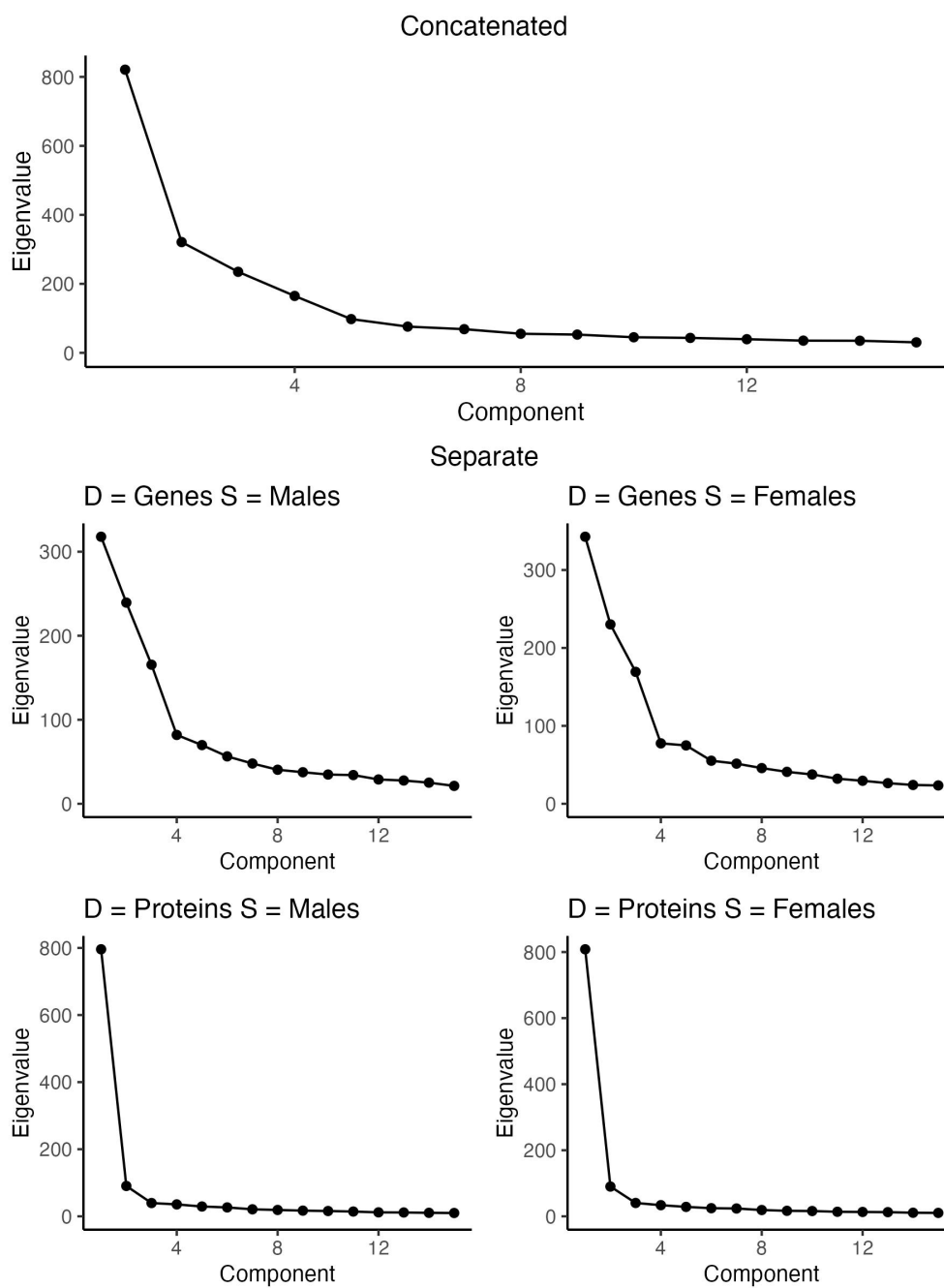


Figure S12: **Computation Time Across 50 COPDGene Data Splits.** Violin plots show the distribution of computation times across the 50 data splits. Comparator methods are fit on each subgroup separately to allow for possible subgroup heterogeneity.

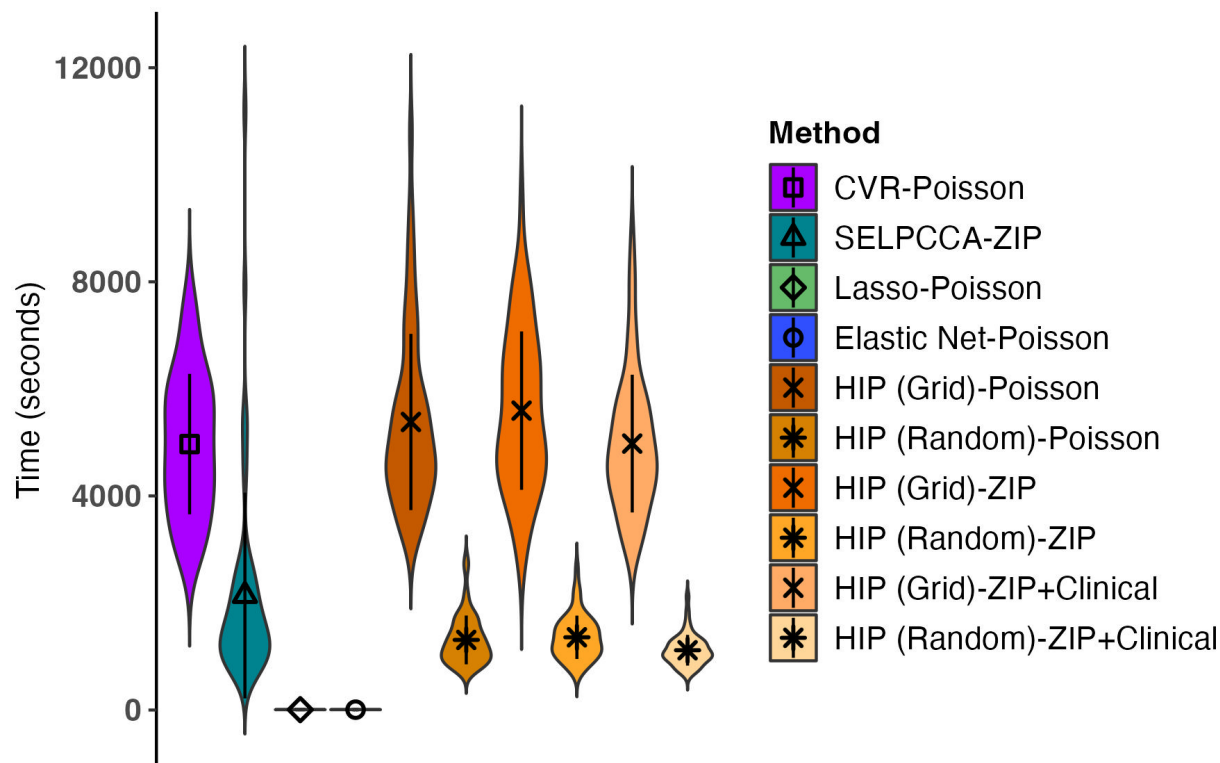


Table S1: **Average Number of Variables Selected Across 50 Test/Train Splits for the COPDGene Data.** Numbers shown are mean (standard deviation). Comparator methods were run without an upper bound on how many variables could be selected. HIP has no variability in the number selected because  $N_{top}$  is specified within each split.

Method	Genes		Proteins	
	Males	Females	Males	Females
CVR-Poisson	210.1 (181.2)	311.1 (125.1)	103.7 (90.3)	103.7 (90.3)
SELPCCA-ZIP	115.1 (168.8)	113.4 (141.9)	73.7 (107.2)	73.7 (107.2)
Lasso-Poisson	113.8 (28.8)	78.8 (43.8)	27.9 (7.3)	27.9 (7.3)
Elastic Net-Poisson	138.3 (20.5)	103.9 (42.2)	34.2 (6.3)	34.2 (6.3)
HIP (Grid)-Poisson	125 (0)	125 (0)	50 (0)	50 (0)
HIP (Random)-Poisson	125 (0)	125 (0)	50 (0)	50 (0)
HIP (Grid)-ZIP	125 (0)	125 (0)	50 (0)	50 (0)
HIP (Random)-ZIP	125 (0)	125 (0)	50 (0)	50 (0)
HIP (Grid)-ZIP+Clinical	125 (0)	125 (0)	50 (0)	50 (0)
HIP (Random)-ZIP+Clinical	125 (0)	125 (0)	50 (0)	50 (0)

Table S2: **Number of Stable Genes and Proteins Selected by Method for the COPDGene Data.** The stable genes and proteins are the top 1% of genes and proteins based on a rank determined by the number of splits the protein/gene entered the model and how many times the protein/gene was selected by the model. The 1% is based on the 5000 genes and 2000 proteins from the unsupervised filtering.

Method	Genes			Proteins		
	Males	Females	Common	Males	Females	Common
CVR-Poisson	50	50	14	21	21	15
SELPCCA-ZIP	50	50	14	20	21	5
Lasso-Poisson	50	50	3	20	20	1
Elastic Net-Poisson	50	51	3	20	20	2
HIP (Grid)-Poisson	51	50	41	20	20	18
HIP (Random)-Poisson	51	50	40	20	20	18
HIP (Grid)-ZIP	51	50	38	20	20	17
HIP (Random)-ZIP	51	50	36	20	20	17
HIP (Grid)-ZIP+Clinical	50	50	33	20	20	18
HIP (Random)-ZIP+Clinical	50	50	36	20	20	17

Table S3: **Number of Stable Genes and Proteins Selected by HIP (Grid)-ZIP and HIP (Random)-ZIP for the COPDGene Data.**

Data	Subtype	Random	Grid	Overlap between Random and Grid
Genes	Males	51	51	49
	Females	50	50	47
	Common	36	38	34
Proteins	Males	20	20	20
	Females	20	20	20
	Common	17	17	17

### 3 HIP Shiny Application Demonstration

#### 3.1 Select Data

The COVID-19 data are from a study that collected blood plasma samples from 102 participants with COVID-19 and 26 participants without COVID-19 to analyze protein, metabolite, RNA-seq, and lipid profiles associated with COVID-19 [1]. Lipman et al. (2022) [2] further analyzed this data to identify ‘stable’ molecules; this pre-processed data are what is included in the *mylearnR* package and available in the Shiny app. The user will need to specify the outcome variable, subgroup variable, and type of outcome. The possible outcomes are number of ventilator free days out of the 45 days enrolled in the study (‘VentFreeDays’), number of hospital free days out of the 45 days enrolled in the study where a zero indicates a patient was either still in the hospital or had died (‘HFD45’), ICU (Intensive Care Unit) status (‘ICU.Status’), and mechanical ventilation status (‘MechVentStatus’). The possible subgroup variables are COVID-19 infection status (‘DiseaseStatus’), biological sex (‘Sex’), ICU status (‘ICU.Status’), and mechanical ventilation status (‘MechVentStatus’). Descriptions of these variables along with links to the papers describing the original study and data pre-processing are included in the right-most column. Note that the same variable should not be specified for both the subgroup and outcome variable. Figure S14 shows what the ‘Input Data’ section where we want to look at the number of hospital free days as a ZIP outcome using COVID-19 status as the subgroup variable.

The user would then click the ‘Submit Data’ button in the left column. This will (1) generate a data summary below the ‘Input Data’ row (Figure S15), (2) create a ‘Download Data’ button below the ‘Submit Data’ button (visible in Figure S14), and (3) populate the ‘K Selection’ row (Figure S16).

#### 3.2 K selection

The scree plot for the concatenated data is shown in Figure S16. The automatic approach suggests using  $K = 1$  for the concatenated data and for each separate  $X^{d,s}$ . The scree plots for the separate  $X^{d,s}$  can be viewed by selecting the desired view and subgroup using the radio buttons in the left column. The threshold for the automatic approach can also be changed here.

Figure S13: **Overlap of Stable Genes and Proteins in the COPDGene Data.** Counts (percents) show how many stable genes and proteins were selected by one or more methods. For example, 10 genes were selected for males by both HIP and SELPCCA.

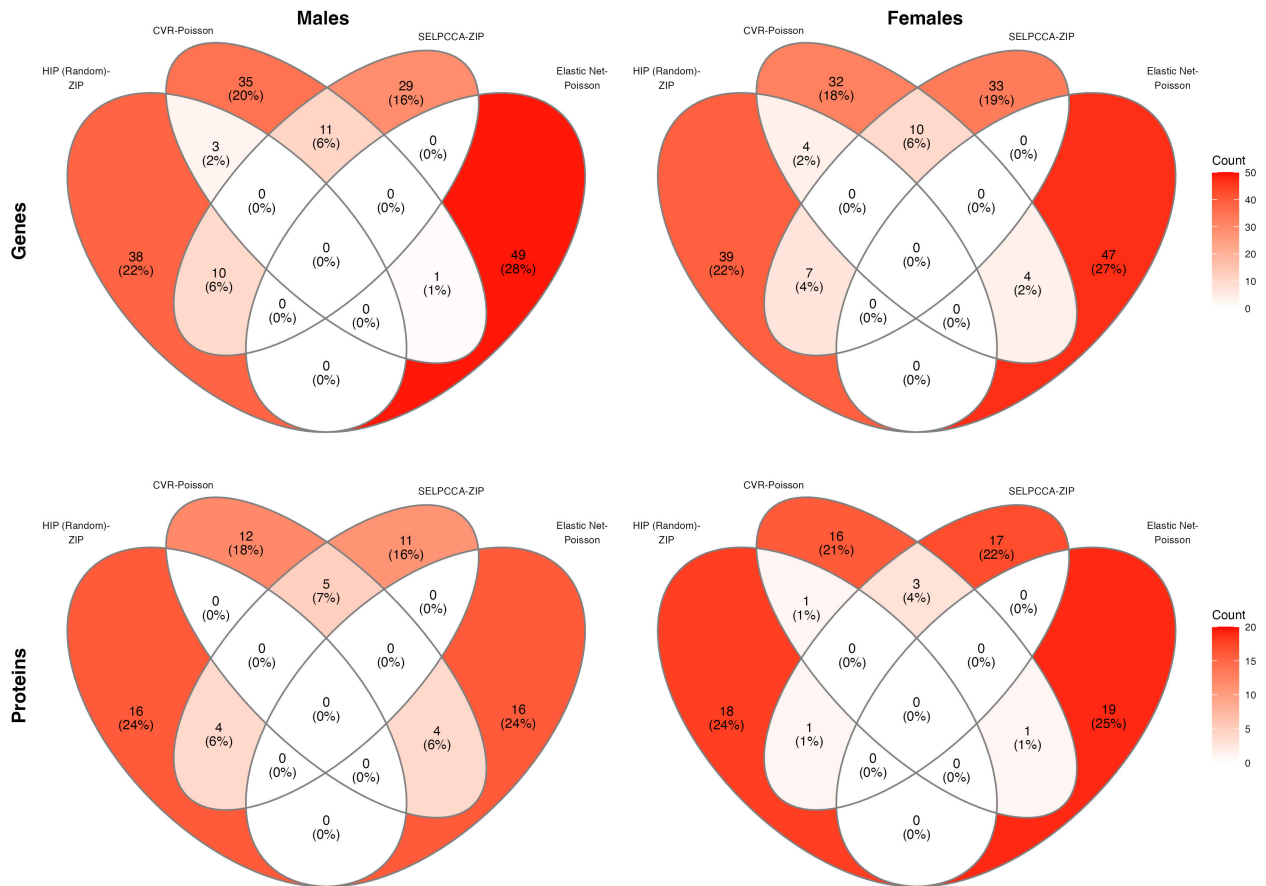


Figure S14: **Example Data Set-up using COVID-19 Data**

### Input Data

**Select the source of your data:**

Upload my own data

Simulate data

Covid data

Click 'Submit Data' once data details have been entered.

**Outcome Variable**

HFD45

**Subgroup Variable**

DiseaseStatus

**Type of Outcome**

ZIP

**Description of Variables**

- HFD45** : Number of hospital free days out of the 45 days enrolled in the study; A zero indicates the patient was either still in the hospital or died.
- VentFreeDays** : Number of ventilator free days out of the 45 days enrolled in the study
- ICU.Status** : Intensive Care Unit status
- MechVentStatus** : Mechanical ventilation status
- DiseaseStatus** : COVID-19 infection status
- Sex** : Biological sex

[Overmeyer et al. \(2021\) \[Source of Data\]](#)

[Lipman et al. \(2022\) \[Preprocessing of Data\]](#)

Table S4: **Stable Genes Selected by HIP (Random) for Males in the COPDGene Data.** Weights are averages from the estimated  $B^{d,s}$  matrices from the subset fit where the variable was selected. Higher values suggest the variable likely contributes more to association and prediction.

ID	Symbol	Weight
ENSG00000100325.15	ASCC2	2.969
ENSG00000167671.12	UBXN6	2.966
ENSG00000136842.14	TMOD1	2.957
ENSG00000259671.1	MTCYBP23	2.948
ENSG00000197081.16	IGF2R	2.932
ENSG00000073792.16	IGF2BP2	2.902
ENSG00000137216.19	TMEM63B	2.897
ENSG00000101236.17	RNF24	2.893
ENSG00000259600.2	RP11_925D83	2.880
ENSG00000259379.1	MTND5P32	2.877
ENSG00000215244.3	LINC02649	2.870
ENSG00000179262.10	RAD23A	2.869
ENSG00000198858.10	R3HDM4	2.866
ENSG00000143774.17	GUK1	2.848
ENSG00000158856.18	DMTN	2.836
ENSG00000287771.1	AC007271.1	2.833
ENSG00000249138.1	SLED1	2.822
ENSG00000137198.10	GMPR	2.810
ENSG00000259626.2	MTND3P12	2.804
ENSG00000103342.13	GSPT1	2.801
ENSG00000090013.11	BLVRB	2.798
ENSG00000168785.8	TSPAN5	2.798
ENSG00000234292.3	AC123595.1	2.793
ENSG00000130830.15	MPP1	2.781
ENSG00000251441.3	RTEL1P1	2.776
ENSG00000143416.21	SELENBP1	2.771
ENSG00000197405.8	C5AR1	2.769
ENSG00000142453.12	CARM1	2.768
ENSG00000102145.15	GATA1	2.768
ENSG00000141084.11	RANBP10	2.763
ENSG00000100614.18	PPM1A	2.757
ENSG00000090238.12	YPEL3	2.753
ENSG00000232334.1	RP11_47G112	2.749
ENSG00000063854.13	HAGH	2.745
ENSG00000185883.12	ATP6V0C	2.745
ENSG00000140564.13	FURIN	2.716
ENSG00000159346.13	ADIPOR1	2.701
ENSG00000257335.8	MGAM	2.678
ENSG00000137193.14	PIM1	2.660
ENSG00000158828.8	PINK1	2.657
ENSG00000100558.9	PLEK2	2.657
ENSG00000182512.5	GLRX5	2.628
ENSG00000135083.16	CCNJL	2.626
ENSG00000166825.15	ANPEP	2.579
ENSG00000068971.14	PPP2R5B	2.573
ENSG00000115590.14	IL1R2	2.566
ENSG00000238005.4	LNCATV	2.550
ENSG00000084110.11	HAL	2.534
ENSG00000185630.19	PBX1	2.531
ENSG00000147454.14	SLC25A37	2.526
ENSG00000119326.15	CTNNA1	2.451



Table S5: **Genes Selected by HIP (Random) for Females for the COPD Gene Data.** Weights are averages from the estimated  $B^{d,s}$  matrices from the subset fit where the variable was selected. Higher values suggest the variable likely contributes more to association and prediction.

ID	Symbol	Weight
ENSG00000158856.18	DMTN	3.521
ENSG00000167671.12	UBXN6	3.463
ENSG00000137216.19	TMEM63B	3.457
ENSG00000004939.15	SLC4A1	3.421
ENSG00000130830.15	MPP1	3.397
ENSG00000115594.12	IL1R1	3.375
ENSG00000100325.15	ASCC2	3.366
ENSG00000090013.11	BLVRB	3.357
ENSG00000198858.10	R3HDM4	3.355
ENSG00000259671.1	MTCYBP23	3.327
ENSG00000063854.13	HAGH	3.325
ENSG00000158578.21	ALAS2	3.323
ENSG00000179262.10	RAD23A	3.310
ENSG00000137198.10	GMPR	3.307
ENSG00000101236.17	RNF24	3.303
ENSG00000241860.7	LOC100996442	3.296
ENSG00000073792.16	IGF2BP2	3.293
ENSG00000135636.14	DYSF	3.275
ENSG00000141084.11	RANBP10	3.245
ENSG00000197405.8	C5AR1	3.241
ENSG00000102145.15	GATA1	3.240
ENSG00000260528.5	FAM157C	3.226
ENSG00000143774.17	GUK1	3.214
ENSG00000259600.2	RP11_925D83	3.207
ENSG00000197081.16	IGF2R	3.204
ENSG00000170315.14	UBB	3.203
ENSG00000287771.1	AC007271.1	3.184
ENSG00000159346.13	ADIPOR1	3.183
ENSG00000090238.12	YPEL3	3.181
ENSG00000185883.12	ATP6V0C	3.173
ENSG00000251441.3	RTEL1P1	3.166
ENSG00000259379.1	MTND5P32	3.142
ENSG00000259626.2	MTND3P12	3.136
ENSG00000060138.13	YBX3	3.132
ENSG00000257335.8	MGAM	3.128
ENSG00000232334.1	RP11_47G112	3.125
ENSG00000137193.14	PIM1	3.110
ENSG00000182512.5	GLRX5	3.102
ENSG00000249138.1	SLED1	3.092
ENSG00000234292.3	AC123595.1	3.088
ENSG00000232528.3	LOC100289473	3.085
ENSG00000215244.3	LINC02649	3.078
ENSG00000135083.16	CCNJL	3.065
ENSG00000167286.10	CD3D	3.035
ENSG00000147454.14	SLC25A37	2.988
ENSG00000084110.11	HAL	2.808
ENSG00000185031.6	SLC2A3P2	2.745
ENSG00000258111.1	RP11_43D42	2.720
ENSG00000137876.11	RSL24D1	2.678
ENSG00000271204.1	RP11_138A91	2.537

Table S6: **Stable Proteins Selected by HIP (Random) for the COPDGene Data.** Weights are averages from the estimated  $B^{d,s}$  matrices from the subset fit where the variable was selected. Higher values suggest the variable likely contributes more to association and prediction.

Subgroup	Name	Symbol	Weight
Males	SHC-transforming protein 1:Src Homology domain	SHC1	3.174
	Amyloid beta A4 protein	APP	3.062
	Neutrophil-activating peptide 2	PPBP	3.031
	Connective tissue-activating peptide III	PPBP	3.022
	UDP-glucuronosyltransferase 2A1	UGT2A1	3.021
	SPARC	SPARC	3.008
	Heparin-binding EGF-like growth factor	HBEGF	3.003
	Platelet-derived growth factor subunit A	PDGFA	2.981
	Thrombospondin-1	THBS1	2.899
	Platelet basic protein	PPBP	2.886
	Endoplasmic reticulum resident protein 44	ERP44	2.809
	Beta-thromboglobulin	PPBP	2.782
	B-cell antigen receptor complex-associated protein alpha chain	CD79A	2.742
	Platelet-derived growth factor subunit B	PDGFB	2.742
	Brain-derived neurotrophic factor	BDNF	2.738
	Tudor-interacting repair regulator protein	NUDT16L1	2.702
	Collagen type IV alpha-3-binding protein:StAR-related lipid-transfer domain, isoform 2	CERT1	2.679
	C-C motif chemokine 5	CCL5	2.665
	Lysyl oxidase homolog 3	LOXL3	2.641
	Syntaxin-8	STX8	2.420
Females	Amyloid beta A4 protein	APP	3.655
	UDP-glucuronosyltransferase 2A1	UGT2A1	3.558
	Neutrophil-activating peptide 2	PPBP	3.553
	Connective tissue-activating peptide III	PPBP	3.539
	SHC-transforming protein 1:Src Homology domain	SHC1	3.503
	Platelet basic protein	PPBP	3.392
	Platelet-derived growth factor subunit A	PDGFA	3.365
	Glia-derived nexin	SERPINE2	3.362
	SPARC	SPARC	3.353
	WAP four-disulfide core domain protein 13	WFDC13	3.286
	Beta-thromboglobulin	PPBP	3.279
	Heparin-binding EGF-like growth factor	HBEGF	3.257
	Thrombospondin-1	THBS1	3.229
	Collagen type IV alpha-3-binding protein:StAR-related lipid-transfer domain, isoform 2	CERT1	3.182
	Brain-derived neurotrophic factor	BDNF	3.164
	Lysyl oxidase homolog 3	LOXL3	3.072
	Peptidyl-prolyl cis-trans isomerase FKBP7	FKBP7	3.052
	Tudor-interacting repair regulator protein	NUDT16L1	3.025
	Platelet-derived growth factor subunit B	PDGFB	3.000
	Syntaxin-8	STX8	2.845

### 3.3 HIP Parameters

Next, the user will need to specify the parameters to use for HIP. The left column allows the user to choose standardization ('Subgroup' or 'None'),  $K$ ,  $\gamma$ , and  $N_{top}$ . We recommend using 'Subgroup' standardization. The default  $K$  value is based on the  $K$  suggested by the automatic selection approach with a threshold of 0.20. The default  $\gamma$  value is a 1 for all data views, i.e., all data views will be penalized by default.  $N_{top}$  can be specified two ways: using a percentage of the variables in each view ('Percent'; Figure S20) or specifying the number of variables directly ('Count'). Figure S17 specifies subgroup standardization,  $K = 1$ , and keeping 25 variables in view 1 and 75 variables in view 2.

The middle column allows the user to run HIP for a fixed  $\lambda$  value or to search for  $\lambda$ . The right column will show options based on this selection. For a fixed value of  $\lambda$ , the user simply enters the desired values for each of  $\lambda_\xi$  and  $\lambda_G$  (Figure S19). This can be used to test upper and lower bounds for a later search for optimal tuning parameters if desired. To search for  $\lambda$ , the user will need to select either a grid or random search, the selection criterion, the number of steps in the grid, and the tuning range to search over (lower and upper bounds). The grid search includes  $num\_steps^2$  combinations of  $\lambda_\xi$  and  $\lambda_G$ , and the random search will select 20% of those combinations. The number of steps and range will be the same for both  $\lambda_\xi$  and  $\lambda_G$ . The default will be to perform a random search from a grid with 8 steps over a  $(0, 2]$  range using  $eBIC_0$  as the selection criterion. Additionally, the user can specify the number of cores to use in the computations; the default is one less than the available cores.

Figure S15: Example Summary of Uploaded Data

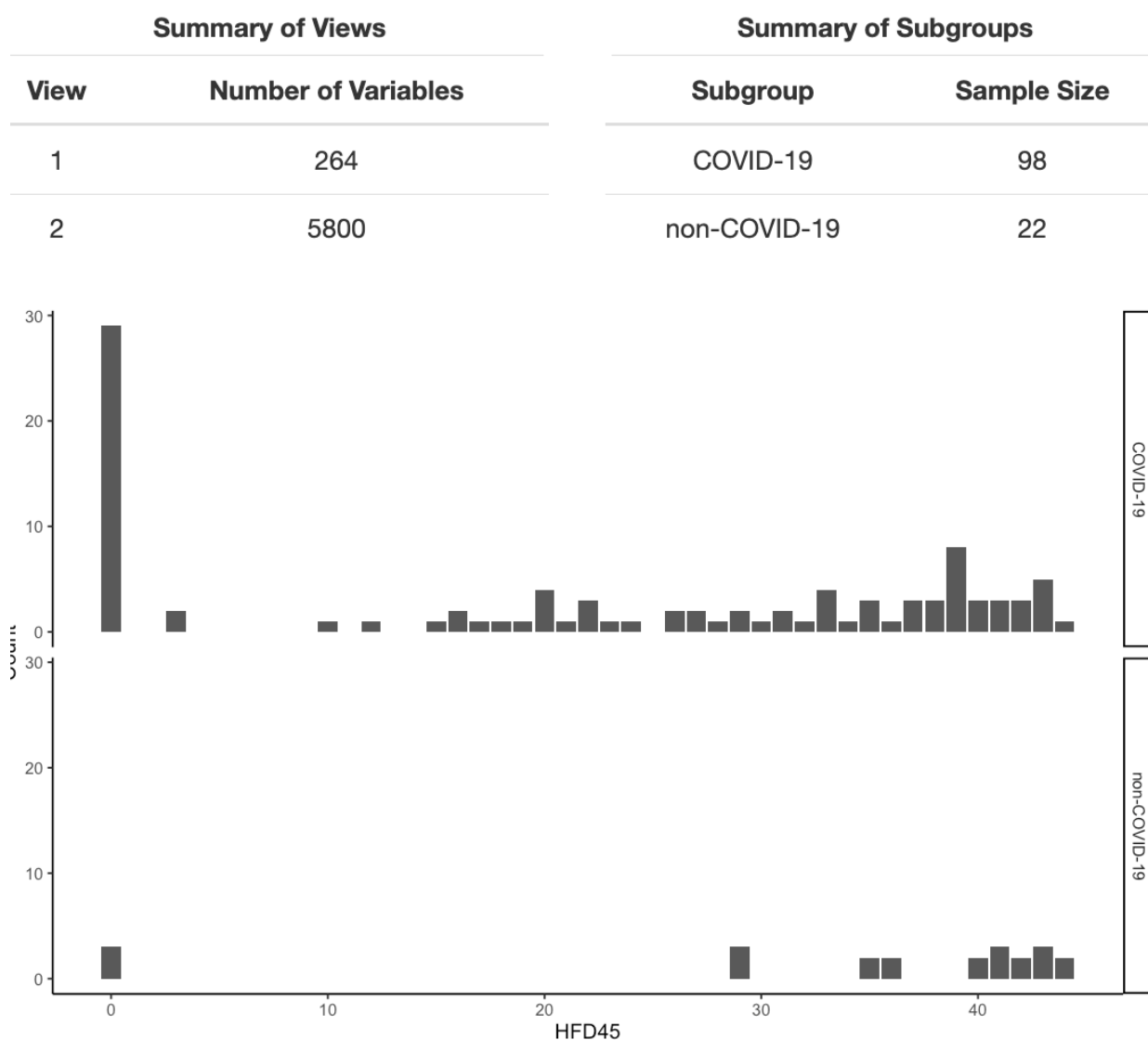


Figure S17 specifies a search to select  $\lambda$ ; it will use a random search using 8 steps from 0 to 2 for each of  $\lambda_\xi$  and  $\lambda_G$ . The analysis will use 7 cores to parallelize the different  $\lambda$  combinations. Once the parameters are set, the user will start the analysis by going to the ‘Results’ tab and clicking the ‘Run Analysis’ button.

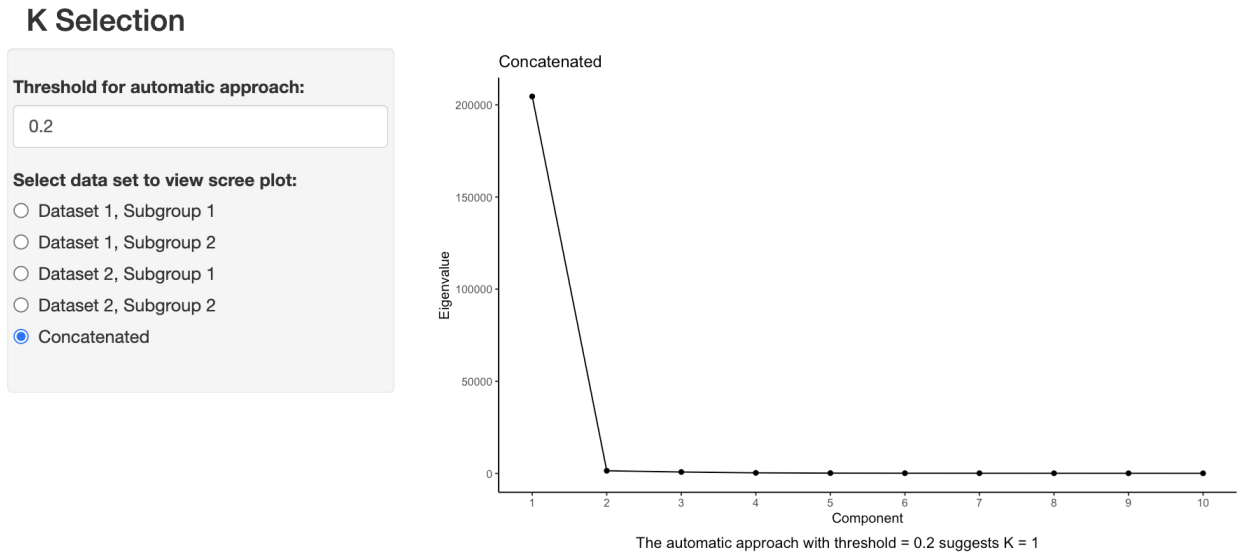
### 3.4 Results

Once the ‘Run Analysis’ button has been clicked, a progress notification (Figure S23) will appear in the lower right corner of the screen so the user knows the analysis has started. The user will know the analysis is complete when the progress notification disappears and the run time is displayed to the right of the ‘Run Analysis’ button.

#### 3.4.1 Result Summary

After the analysis is complete, the left column in the ‘Result Summary’ section will provide a button to download results, and the right column will display some basic information about the results for the user including the convergence status, the  $\lambda$  values used, the  $eBIC_1$  or other selection criterion value, the run time, and the applicable training prediction metric. Figure S24 shows this summary for this COVID-19 demonstration. The downloaded results will contain the values of the estimated  $B^{d,s}$  matrices along with summary information.

Figure S16: K Selection Demonstration



### 3.4.2 Prediction and Performance

The next section displays the applicable prediction metric for the training data and the test data if they are available. If there are no test data available, a message will be printed for the user stating so. The prediction metric is the mean squared error for Gaussian outcomes, classification accuracy for multi-class outcomes, and fraction of deviance explained for Poisson and ZIP outcomes. The appropriate metric and formula are displayed in a gold box in the left column for users. Figure S25 shows the training fraction of deviance explained for our analysis and prints a message that no test data is available.

### 3.4.3 Variable importance

The weights from the estimated  $B^{d,s}$  matrices are displayed in two formats. The first is a variable importance plot that includes all variables that were included in the subset model fit (Figure S26). The variables are ranked based on the weights within each view and subgroup. The plots are generated with R package `ggplot` [3] for each subgroup and view and then combined into a single figure using R package `ggpubr` [4].

The second output is an interactive table with columns for the rank (within view and subgroup), variable, weight, view, and subgroup (Figure S27). This table can be sorted by or filtered on any column so that the user can explore the results. Some possible options that could be of interest include selecting the top ranked variable(s) for each view and subgroup, selecting a specific variable to compare between subgroups, or selecting all results for a single view and subgroup (Figures S28, S29, and S30). This table is generated using the R package `DT` [5].

Figure S17: Demonstration of Setting HIP Parameters

## HIP Parameters

**Select what standardization to apply to your data:**

For Gaussian outcomes, standardization will be applied to X and Y. For all other outcomes, standardization will only be applied to X.

- Subgroup  
 None

**Select a value for K:**

Default value is the K chosen by the automatic approach on the concatenated data with threshold = 0.20

**Enter values for  $\gamma$ :**

Must be length D. Values should be 1 (include penalty on view) or 0 (no penalty on view).

**Select how to specify  $N_{top}$ :**

Percent keeps the same percentage of variables for each view. Count specifies the exact number of variables for each view.

- Percent  
 Count

**Number of variables to keep:**

If you enter a single integer, that will be used for all views. For different values in each view, enter a comma separated list of length D.

**How do you want to run HIP?**

- For a fixed  $\lambda$   
 Search for  $\lambda$

**Select the type of search:**

Grid will search all  $\lambda$  combinations. Random will search 20% of the combinations.

- Grid  
 Random

**Selection Criterion:**

Further options for "Information Criterion" will be displayed in the "Results" tab.

- Information Criterion  
 5-fold CV

**Number of Steps:**

Default = 8

**Search Range Minimum:**

Applies to both  $\lambda_\varepsilon$  and  $\lambda_G$ . Default = 0.0

**Search Range Maximum:**

Applies to both  $\lambda_\varepsilon$  and  $\lambda_G$ . Default = 2.0

**Number of cores to use:**

Default is available cores - 1.

Figure S18: **HIP Parameter Options**Figure S19: Fixed  $\lambda$ 

**How do you want to run HIP?**

For a fixed lambda

Search for lambda

**Value for  $\lambda_\xi$**

Default = 1.0

**Value for  $\lambda_G$**

Default = 1.0

Figure S20:  $N_{top}$  Specified by Percent

**Select how to specify  $N_{top}$  :**

Percent keeps the same percentage of variables for each view. Count specifies the exact number of variables for each view.

Percent

Count

**Percent of variables to keep:**

Default = 10%

1

10

100

1
11
21
31
41
51
61
71
81
91
100

Figure S21: **Start Analysis** (a) To start the analysis, users click this button. (b) The progress notification that appears while the analysis is running.

Figure S22: Button to Start Analysis

## Start Analysis

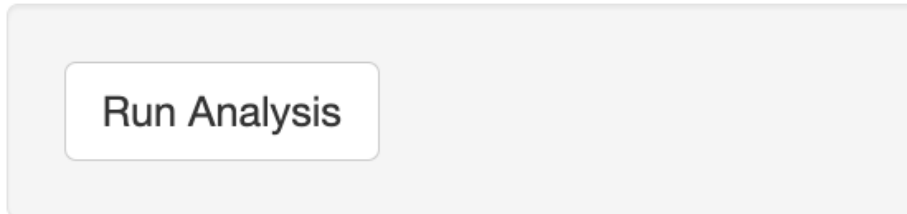


Figure S23: Progress Notification

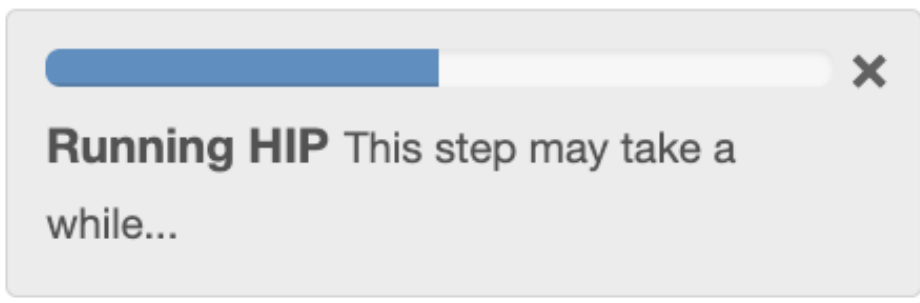
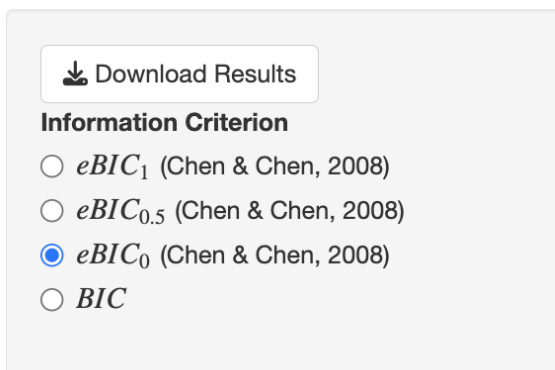


Figure S24: **Example Result Summary**

## Result Summary



### Results from best fit selected using $eBIC_0$ :

Full Model Convergence Status: Converged  
 Subset Model Convergence Status: Converged  
 Selected  $\lambda$ : 2, 2  
 Value of selection criterion = 2408.599  
 Training Fraction of Deviance Explained = 0.415

Figure S25: Example Prediction and Performance Results

## Prediction and Performance

Value is fraction of deviance explained ( $D^2$ ).

$$D^2 = \frac{D_{null} - D_{opt}}{D_{null}}$$

**Train**

0.415

**Test**

No test data available.

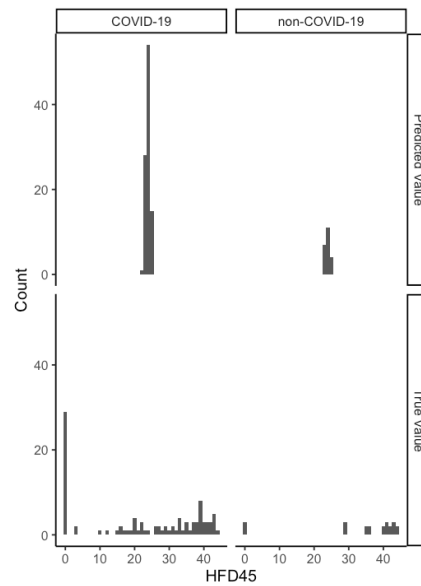
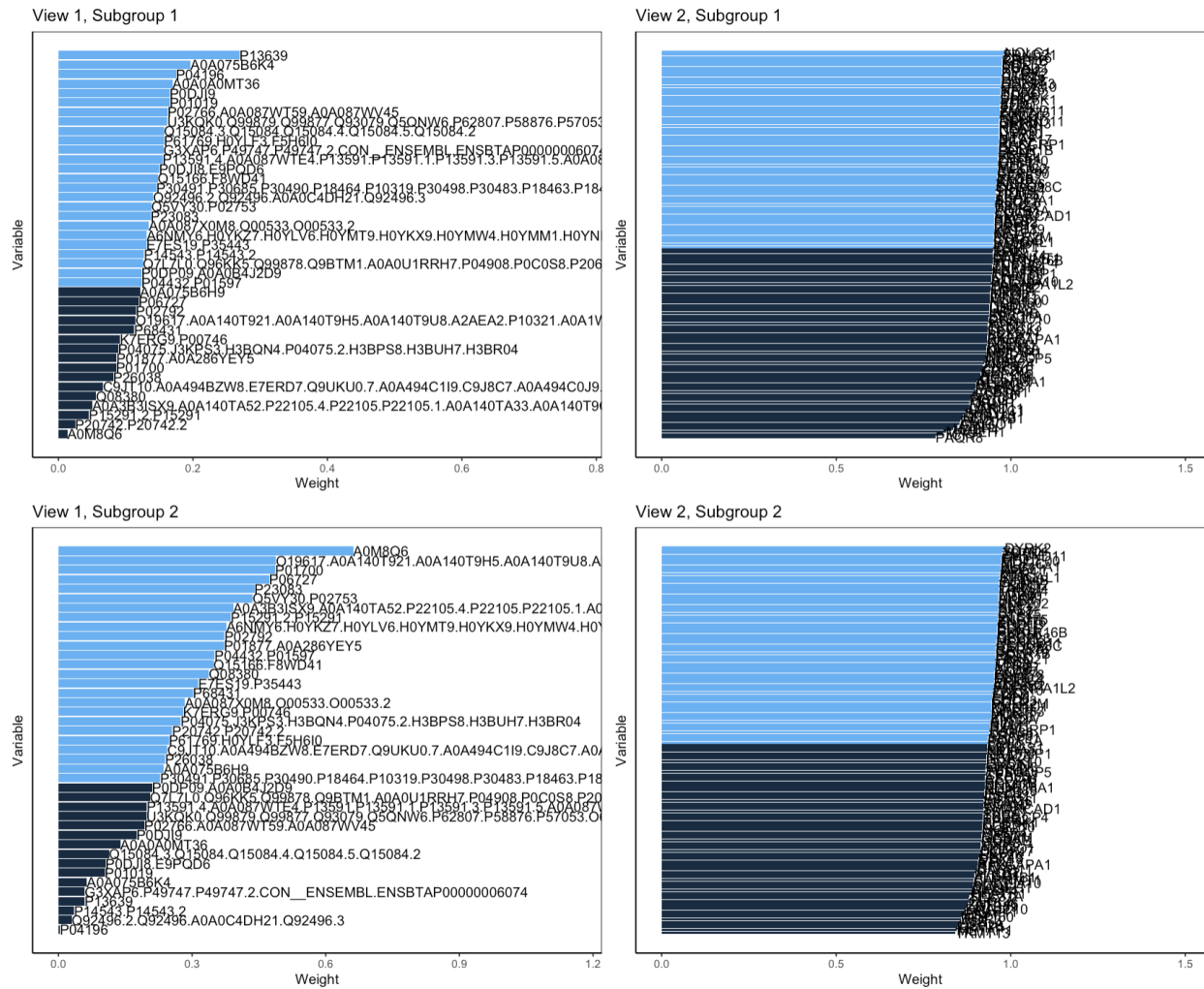




Figure S26: Example Variable Importance Plot

Variable Importance Plot



Note: Light blue fill indicates the variable is in  $N_{top}$  for that view and subgroup.

Figure S27: Example Variable Importance Table.

**Variable Importance Table**

Show  entries Search:

Rank	Weight	Variable	View	Subgroup
<input type="text" value="All"/>	<input type="text" value="All"/>	<input type="text" value="All"/>	<input type="text" value="All"/>	<input type="text" value="All"/>
1	0.2697	P13639	1	1
2	0.1966	A0A075B6K4	1	1
3	0.175	P04196	1	1
4	0.17	A0A0A0MT36	1	1
5	0.1656	P0DJI9	1	1
6	0.1654	P01019	1	1
7	0.1623	P02766.A0A087WT59.A0A087WV45	1	1
8	0.162	U3KQK0.Q99879.Q99877.Q93079.Q5QNW6.P62807.P58876.P57053.O60814.Q5QNW6.2.Q99880.Q96A08	1	1
9	0.157	P61769.HOYLF3.F5H6I0	1	1
10	0.157	Q15084.3.Q15084.Q15084.4.Q15084.5.Q15084.2	1	1

Showing 1 to 10 of 376 entries Previous  2 3 4 5 ... 38 Next

Figure S28: Filter on Rank

**Variable Importance Table**

Show  entries Search:

Rank	Weight	Variable	View	Subgroup
<input type="text" value="1 ... 1"/> <input checked="" type="radio"/>	<input type="text" value="All"/>	<input type="text" value="All"/>	<input type="text" value="All"/>	<input type="text" value="All"/>
1	0.2697	P13639	1	1
1	0.6617	A0M8Q6	1	2
1	0.9824	NOLC1	2	1
1	0.983	DYRK2	2	2

Showing 1 to 4 of 4 entries (filtered from 376 total entries) Previous  Next

Figure S29: Filter on Variable Name

**Variable Importance Table**

Show  entries Search:

Rank	Weight	Variable	View	Subgroup
<input type="text" value="All"/>	<input type="text" value="All"/>	<input checked="" type="radio"/> P13639	<input type="text" value="All"/>	<input type="text" value="All"/>
1	0.2697	P13639	1	1
38	0.0589	P13639	1	2

Showing 1 to 2 of 2 entries (filtered from 376 total entries) Previous  Next

Figure S30: Filter on Specific View and Subgroup

**Variable Importance Table**

Show  entries Search:

Rank	Weight	Variable	View	Subgroup
<input type="text" value="All"/>	<input type="text" value="All"/>	<input type="text" value="All"/>	<input type="text" value="2 ... 2"/>	<input type="text" value="1 ... 1"/>
1	0.9824	NOLC1	2	1
2	0.9789	FBXO21	2	1
3	0.9782	ZNHIT6	2	1
4	0.9752	RRP1B	2	1
5	0.9748	KLF12	2	1
6	0.9747	MTR	2	1
7	0.9741	SDAD1	2	1
8	0.9741	XPO4	2	1
9	0.9738	DYRK2	2	1
10	0.9736	UTP25	2	1

Showing 1 to 10 of 147 entries (filtered from 376 total entries) Previous  2 3 4 5 ... 15 Next

## References

- [1] Katherine A. Overmyer, Evgenia Shishkova, Ian J. Miller, Joseph Balnis, Matthew N. Bernstein, Trenton M. Peters-Clarke, Jesse G. Meyer, Qiuwen Quan, Laura K. Muehlbauer, Edna A. Trujillo, Yuchen He, Amit Chopra, Hau C. Chieng, Anupama Tiwari, Marc A. Judson, Brett Paulson, Dain R. Brademan, Yunyun Zhu, Lia R. Serrano, Vanessa Linke, Lisa A. Drake, Alejandro P. Adam, Bradford S. Schwartz, Harold A. Singer, Scott Swanson, Deane F. Mosher, Ron Stewart, Joshua J. Coon, and Ariel Jaitovich. Large-scale multi-omic analysis of covid-19 severity. *Cell Systems*, 12(1):23–40.e7, 2021. doi:10.1016/j.cels.2020.10.003. URL <https://doi.org/10.1016/j.cels.2020.10.003>.
- [2] Danika Lipman, Sandra E. Safo, and Thierry Chekouo. Multi-omic analysis reveals enriched pathways associated with covid-19 and covid-19 severity. *PLOS ONE*, 17(4):1–30, 04 2022. doi:10.1371/journal.pone.0267047. URL <https://doi.org/10.1371/journal.pone.0267047>.
- [3] Hadley Wickham. *ggplot2: Elegant Graphics for Data Analysis*. Springer-Verlag New York, 2016. ISBN 978-3-319-24277-4. URL <https://ggplot2.tidyverse.org>.
- [4] Alboukadel Kassambara. *ggpubr: 'ggplot2' Based Publication Ready Plots*, 2023. URL <https://CRAN.R-project.org/package=ggpubr>. R package version 0.6.0.
- [5] Yihui Xie, Joe Cheng, and Xianying Tan. *DT: A Wrapper of the JavaScript Library 'DataTables'*, 2023. URL <https://CRAN.R-project.org/package=DT>. R package version 0.28. 28